Fuel-Flexible Gasification-Combustion Technology for Production of H_2 and Sequestration-Ready CO_2

Annual Technical Progress Report 2002

Reporting Period:

October 1, 2001 – September 30, 2002

George Rizeq, Janice West, Arnaldo Frydman, Raul Subia, and Vladimir Zamansky (GE EER)
Hana Loreth, Lubor Stonawski, Tomasz Wiltowski, Edwin Hippo, and Shashi Lalvani (SIU-C)

October 2002

DOE Award No. DE-FC26-00FT40974

General Electric Energy and Environmental Research Corporation
(GE EER)
18 Mason
Irvine, CA 92618

DISCLAIMER

ABSTRACT

It is expected that in the 21st century the Nation will continue to rely on fossil fuels for electricity, transportation, and chemicals. It will be necessary to improve both the thermodynamic efficiency and environmental impact performance of fossil fuel utilization. GE Energy and Environmental Research Corporation (GE EER) has developed an innovative fuel-flexible Advanced Gasification-Combustion (AGC) concept to produce H_2 and sequestration-ready CO_2 from solid fuels. The AGC module offers potential for reduced cost and increased energy efficiency relative to conventional gasification and combustion systems. GE EER was awarded a Vision 21 program from U.S. DOE NETL to develop the AGC technology. Work on this three-year program started on October 1, 2000. The project team includes GE EER, California Energy Commission, Southern Illinois University at Carbondale, and T. R. Miles, Technical Consultants, Inc.

In the AGC technology, coal/opportunity fuels and air are simultaneously converted into separate streams of (1) pure hydrogen that can be utilized in fuel cells, (2) sequestration-ready CO_2, and (3) high temperature/pressure oxygen-depleted air to produce electricity in a gas turbine. The process produces near-zero emissions and, based on preliminary modeling work, has an estimated process efficiency of approximately 67% based on electrical and H_2 energy outputs relative to the higher heating value of coal. The three-year R&D program will determine the operating conditions that maximize separation of CO_2 and pollutants from the vent gas, while simultaneously maximizing coal conversion efficiency and hydrogen production. The program integrates lab-, bench- and pilot-scale studies to demonstrate the AGC concept.

This is the second annual technical progress report for the Vision 21 AGC program supported by U.S. DOE NETL (Contract No. DE-FC26-00FT40974). This report summarizes program accomplishments for the period starting October 1, 2001 and ending September 30, 2002. The report includes an introduction summarizing the AGC concept, main program tasks, and program objectives; it also provides a summary of program activities and accomplishments covering progress in tasks including lab- and bench-scale experimental testing, pilot-scale design and assembly, and program management.

TABLE OF CONTENTS

LIST OF TABLES

LIST OF FIGURES

LIST OF ACRONYMS

A	Frequency factor
AGC	Advanced gasification-combustion
CAM	CO_2 absorber material
CEC	California Energy Commission
CTQ	Critical to quality
DFSS	Design for six sigma
E_a	Activation energy
GE EER	General Electric Energy and Environmental Research Corporation
IGCC	Integrated gasification combined cycle
NETL	National Energy Technology Laboratory
NTI	New technology introduction
OD	Outside diameter
OTM	Oxygen transfer material
P&ID	Process and instrumentation diagram
R1	Reactor 1
R2	Reactor 2
R3	Reactor 3
SIU-C	Southern Illinois University – Carbondale
SS	Stainless steel
U.S. DOE	United States Department of Energy

1.0 INTRODUCTION

Electricity produced from hydrogen in fuel cells can be highly efficient relative to competing technologies and has the potential to be virtually pollution free. Thus, fuel cells may become an ideal solution to many of this nation's energy needs if one has a satisfactory process for producing hydrogen from available energy resources such as coal, and low-cost alternative feedstocks including biomass, municipal solid waste, sewage sludge, and others.

This Vision 21 program addresses a novel, energy-efficient, and near-zero pollution concept for converting a conventional fuel (coal) and opportunity fuels (e.g., biomass) into separate streams of hydrogen, oxygen-depleted air, and sequestration-ready CO_2. This concept is referred to throughout this report as *Advanced Gasification-Combustion (AGC)*. When commercialized, the AGC process may become one of the cornerstone technologies to fulfill Vision 21 energy plant objectives of efficiently and economically producing energy and hydrogen with utilization of opportunity feedstocks.

The AGC technology is energy efficient because a large portion of the energy in the input coal leaves the AGC module as hydrogen and the rest as high-pressure, high-temperature gas that can power a gas turbine. The combination of producing hydrogen and electrical power via a gas turbine is highly efficient, meets all objectives of Vision 21 energy plants, and makes the process flexible. That is, the AGC module will be able to adjust the ratio at which it produces hydrogen and electricity in order to match changing demand.

The three-year Vision 21 AGC program is being conducted primarily by General Electric Energy and Environmental Research Corporation (GE EER) under a Vision 21 contract from U.S. DOE NETL (Contact No. DE-FC26-00FT40974). Other project team members include Southern Illinois University at Carbondale (SIU-C), California Energy Commission (CEC), and T. R. Miles, Technical Consultants, Inc. The AGC project integrates lab-, bench- and pilot-scale studies to demonstrate the AGC concept. Engineering studies and analytical modeling will be performed in conjunction with the experimental program to develop the design tools necessary for scaling up the AGC technology to the demonstration phase. The remainder of this section presents objectives, concept, and main tasks of the AGC program.

1.1 Program Objectives

The primary objectives of the AGC program are to:

- Demonstrate and establish the chemistry of the AGC concept, measure kinetic parameters of individual process steps, and identify fundamental processes affecting process economics.
- Design and develop bench- and pilot-scale systems to test the AGC concept under dynamic conditions and estimate the overall system efficiency for the design.
- Develop kinetic and dynamic computational models of the individual process steps.
- Determine operating conditions that maximize separation of CO_2 and pollutants from vent gas, while simultaneously maximizing coal/opportunity fuels conversion and H_2 production.
- Integrate the AGC module into Vision 21 plant design and optimize work cycle efficiency.
- Determine extent of technical/economical viability & commercial potential of AGC module.

1.2 AGC Concept

The conceptual design of the AGC technology is depicted in Figure 1-1. The AGC technology makes use of three circulating fluidized bed reactors containing CO_2 absorbing material (CAM) and oxygen transfer material (OTM), as shown in Figure 1-1. Coal and some opportunity fuels (5-10% by heat input) are partially gasified with steam in the first reactor, producing H_2, CO and CO_2. As CO_2 is absorbed by the CO_2 sorbent, CO is also depleted from the gas phase via the water-gas shift reaction. Thus, the first reactor produces a H_2-rich product stream suitable for use in liquefaction, fuel cells, or turbines.

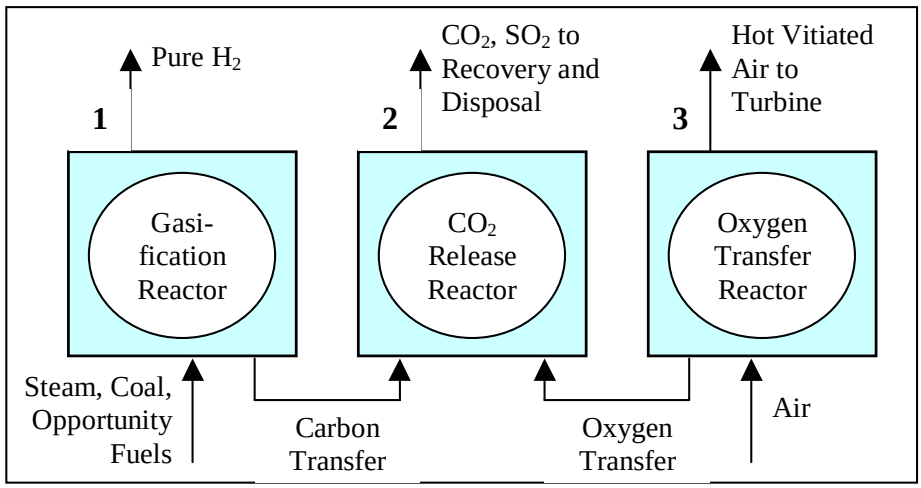

Figure 2-1. Conceptual design of the AGC technology.

Gasification of the char, transferred from the first reactor, is completed with steam fluidization in the second reactor. The oxygen transfer material is reduced as it provides the oxygen needed to oxidize CO to CO_2 and H_2 to H_2O. The CO_2 sorbent is regenerated as the hot moving material from the third reactor enters the second reactor. This increases the bed temperature forcing the release of CO_2 from the sorbent, generating a CO_2-rich product stream suitable for sequestration.

Air fed to the third reactor re-oxidizes the oxygen transfer material via a highly exothermic reaction that consumes the oxygen in the air fed. Thus, reactor three produces oxygen-depleted air for a gas turbine as well as generating heat that is transferred to the first and second reactors via solids transfer.

Solids transfer occurs between all three reactors, allowing for the regeneration and recirculation of both the CO_2 sorbent and the oxygen transfer material. Periodically, ash and bed materials will be removed from the system and replaced with fresh bed materials to reduce the amount of ash in the reactor and increase the effectiveness of the bed materials.

1.3 Project Plan

The tasks planned for the AGC project are summarized in Table 1-1. These tasks are being conducted over the three-year period that started October 1, 2000. The success of the AGC program depends on the efficient execution of the various research tasks outlined in Table 1-1 and on meeting the program objectives summarized above.

2.0 PROGRAM PLANNING AND MANAGEMENT

Program planning activities have focused on meeting the objectives of the program as stated previously. GE EER has made use of several GE methodologies to obtain desired results and systematically conduct program design, construction and testing activities. Methodologies utilized in this program include New Technology Introduction (NTI) and Design For Six Sigma (DFSS). The NTI program is a detailed and systematic methodology used by GE to identify market drivers, and continually ensure that the program will meet both current and future market needs. The NTI program is also strongly coupled with the DFSS and other quality programs, providing structure to the design process and ensuring that the design meets program objectives. This is accomplished through regular program reviews, detailed design reviews, market assessments, planning and decision tools, and specific quality projects aimed at identifying system features and attributes that are critical to quality (CTQ) for customers.

Table 2-1. Main tasks of the AGC program.

Task	Task Description
Lab-Scale Experiments – Fundamentals *Task 1*	Design & assembly Demonstration of chemical processes Sulfur chemistry
Bench-Scale Test Facility & Testing *Tasks 2 & 3*	Bench test facility design Subsystems procurement& assembly Bench test facility shakedown Reactor design testing Parametric evaluation Fuel-flexibility evaluation Pilot operation support
Engineering & Modeling Studies *Task 4*	Opportunity fuels resource assessment Preliminary economic assessment Kinetic & process modeling Integration into Vision 21 plant Pilot plant control development
Pilot Plant Design, Assembly & Demonstration *Tasks 5, 6, & 7*	Process design Subsystems specification/procurement Reactor design & review Reactors manufacture Components testing Pilot plant assembly Operational shakedown modifications Operational evaluation Fuel-flexibility evaluation Performance testing
Vision 21 Plant Systems Analysis *Task 8*	Preliminary Vision 21 module design Vision 21 plant integration Economic & market assessment
Project Management *Task 9*	Management, reporting, & technology transfer

The project team meets weekly to assess progress, distribute workload, and identify and remove potential roadblocks. An expanded NTI project team that includes senior management and other expert personnel also meets biweekly to gauge progress and ensure that company resources are allocated and technical issues resolved to allow steady progress toward program objectives. Another purpose of the biweekly NTI meeting is to ensure that the technology is developed in a manner that continues to allow it to meet emerging market needs by following the GE NTI methodology. This includes detailed design reviews as progress is made on system designs.

Program management activities also involve continuous oversight of program expenditures. This includes monthly review of actual expenditures and monthly projections of labor, equipment, contractor costs, and materials costs.

Technology transfer and networking with experts in the advanced power generation field is an important part of project management. During the second program year, team members have presented the AGC concept and progress at several conferences. A list of references for these presentations and publications is provided in Section 10.0 of this report.

During this reporting period, the GE EER Vision 21 team met with Dr. Kamalendu Das (DOE Project Officer) on Feb 4, 2002 at GE EER's corporate offices in Irvine, CA. During the daylong meetings, the Vision 21 AGC engineering team updated Dr. Das with progress on various ongoing tasks in the AGC program including lab, bench, and pilot-scale studies and preliminary economic assessment. Additionally, Dr. Das visited the GE EER Test Site in Irvine and toured the Vision 21 AGC bench-scale set-up and observed experimental activities.

An internal mid-year review of the Vision 21 AGC program progress was held on September 9, 2002 with senior GE management to discuss plans for the demonstration and continued development of the AGC technology. During the review, the team's efforts at integrating the Design for Six Sigma approach were praised, and the consensus was that a detailed plan is in place to meet program technical objectives and GE commercialization objectives.

During the second year of this program, results from the experimental facilities have been obtained, analyzed and used to assess operating characteristics of the system. The laboratory-scale activities are being conducted by SIU in Carbondale, IL, while the bench-scale and pilot-scale (under construction) systems are located at GE EER's test facility in Irvine, CA.

3.0 LABORATORY-SCALE TESTING (Task 1)

The primary objective of Task 1 is to perform a laboratory-scale demonstration of the individual chemical and physical processes involved in GE EER's fuel-flexible AGC technology. Specific objectives of Task 1 include:

- Support bench- and pilot-scale studies;
- Assist in process optimization and engineering analysis;
- Identify key kinetic and thermodynamic limitations of the process; and
- Verify the process parameters at laboratory scale.

Work conducted in the second year of this program has focused on the impact of OTM on coal gasification reaction rates in a fixed bed reactor system. Recent experimental work has provided data from a high-temperature, high-pressure fluidized bed reactor.

3.1 Fixed Bed Experiments

3.1.1 Experimental Method

The effect of OTM addition on coal gasification was studied by analyzing the product gas compositions produced from gasification of a variety of mixtures of Utah coal and OTM. A quartz glass tube reactor with an inner diameter of 1 cm was used as the primary reaction chamber. Glass wool packing material was used to fix the bed position and to facilitate steam

superheating. The basic configuration of the system is shown in Figure 3-1. The reactor was moved into position inside the furnace and steam fed to the system once the desired furnace temperature was achieved. Nitrogen was used as carrier gas for all the experiments. A cold trap was located before the sampling outlet to condense out any tar components. Reaction progress was followed by gas chromatography (Gow-Mac series 600) analysis of product gas samples. Testing was conducted at 800, 850 and 900ºC at atmospheric pressure. The OTM was either mixed with the coal or layered behind the coal, as shown in Figure 3-2.

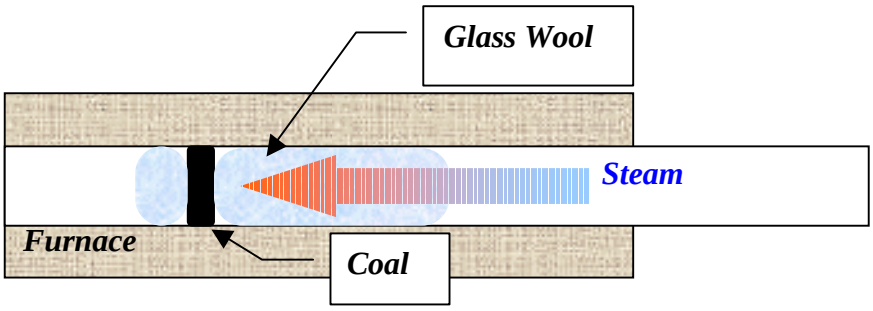

Figure 3-1. Experimental system configuration: relative positions of coal and glass wool packing material.

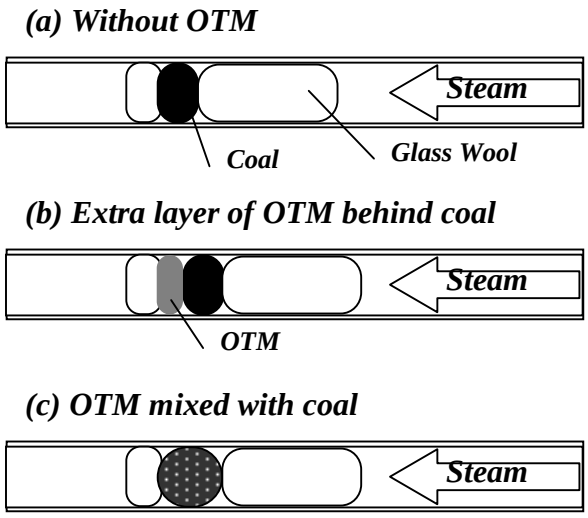

Figure 3-2. Arrangement of OTM relative to coal (layered or mixed).

The reaction rate constants and activation energy of coal gasification (without OTM) were calculated for basic reaction conditions (carrier gas flow rate of 30ml/min, water flow rate of 0.5ml/min, reaction temperature 800ºC or 900ºC). Reaction rate constants were obtained from coal residue measurements. Tests were performed for reaction times of 3, 5 and 10 minutes.

3.1.2 Effect of OTM Addition

The reaction rate constants and activation energy of steam gasification of coal with OTM addition were calculated for basic reaction conditions (carrier gas flow rate of 30 ml/min, water flow rate of 0.5 ml/min, and reaction temperatures of 800°C and 900°C). Results were compared to those obtained from experiments performed with coal only (under same conditions). As indicated above, the OTM added to the reactor was either mixed with coal sample or layered behind the coal sample. The initial OTM mass was 0.065g (4.0×10^{-4} mol) per coal sample (0.2g) for all tests. Coal reactivity was observed to be strongly dependent on both reaction temperature and steam inlet temperature. It was observed that steam flow rates above the instrument-specific limiting flow rate exceeded the capacity of the superheater to bring the steam to reactor temperature; thus, for high steam flow rates, the steam inlet temperature was too low to provide meaningful results. This limitation of the experimental apparatus has been investigated, and experiments have been designed to prevent the use of steam flow rates that result in low steam inlet temperatures.

The gasification reaction with OTM addition was assumed to be a first-order reaction, as in the case of coal only. The relationship between $\ln(C/C_0)$ and reaction time is shown in Figure 3-3, where C_0 is the initial coal sample mass [g] and C is obtained by subtracting the added OTM mass from the residue mass [g]. The calculated rate constants are provided in Table 3-1 based on data from Figure 3-3.

For experiments conducted at 800°C, the rate constant increased slightly for the layered OTM case. The difference in behavior with OTM addition type suggests that different mechanisms are impacting behavior. Specifically, it seems that mixed OTM facilitates the decomposition of coal volatile matter, while layered OTM promotes the decomposition of fixed carbon in coal. However, for experiments at 900°C, OTM addition did not impact the coal decomposition behavior. Thus, the impact of OTM on coal decomposition is most significant at temperatures below 900°C.

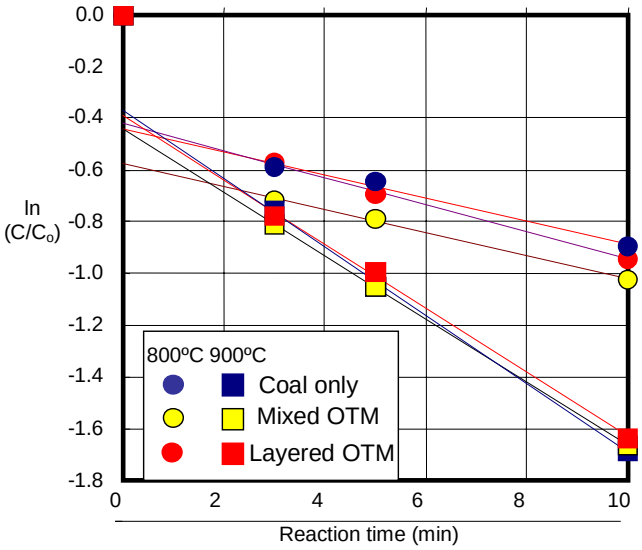

Figure 3-3. First order plot at 800°C and 900°C.

Arrhenius parameters were calculated based on the results provided above and are listed in Table 3-2. The presence of OTM lowered both the activation energy (E_a) and the frequency factor (A). The change in activation energy was especially significant for layered OTM. Confirmation of these observations will be conducted later under fluidized bed conditions in lab-, bench- and pilot-scale experiments.

Table 3-1. Reaction rate constants (min^{-1})

	Furnace Temp. (°C)	
	800	900
Coal only	.0444	.132
Layered OTM	.0523	.124
Mixed OTM	.0446	.122

3.2 Fluidized Bed Experiments

3.2.1 System Design

Table 3-2. Arrhenius parameters.

	E_a (kJ mol^{-1})	A (min^{-1})
Coal only	114.2	16349
Layered OTM	90.0	1259
Mixed OTM	105.1	5820

The high-temperature fluidized bed reactor is a 1-inch diameter schedule 40 Incoloy 800HT pipe fitted with a 1" diameter porous quartz distributor plate. The distributor plate is located near the bottom of the reactor, to allow space for the bed solids as well as for bed expansion. The outlet of the reactor is fitted with a thermocouple that extends down to the bed, as well as port for solids delivery. The bottom of the reactor has two ports for the steam and N_2 inlets. During high-pressure experiments, the reactor is inserted into a 3" pipe with 900-lb flanges that can withstand the high operating pressures. The entire system is heated in an electric furnace. The 3" pipe serves as a preheater for steam, as the reactor is much shorter than the 3" pipe. This also ensures that the fluidized bed is located near the center of the electric furnace.

3.2.2 Experimental Results

Seven experiments were conducted using the fluidized bed reactor. Silica sand (mesh US # 200), washed in acid, was used as the fluidization medium in certain experiments. Description of experimental conditions is summarized in Table 3-3.

Table 3-3. Test matrix for fluidized bed experiments.

Test ID#:	Temp. [^{o}C]	Steam [%]	CAM [g]	OTM [g]	Sand [g]	H_2 produced [ml]
35	670	0	0	0	60	89
36	670	75	0	0	60	286
37	670	75	10	10	40	311
38	670	75	40	10	0	479
39	670	75	40	30	0	336
40	670	75	40	20*	0	164
41	670	50	20	5	25	230

* extra 10 g of OTM was injected with coal

Fluidization solids were inserted into the reactor, which was heated to 700^{o}C under flowing nitrogen at atmospheric pressure. The inner bed temperature was stabilized at 670^{o}C. Steam was introduced into the reactor and the nitrogen flow rate was adjusted to provide a total gas flow rate equal to 15 times the minimum fluidization velocity. Coal (2.5 g in all cases) was injected using the solids delivery system.

Table 3-3 also shows the amount of H_2 produced for each test. The maximum H_2 was achieved during Test #38, with a CAM:OTM ratio of 4:1. The concentration profile for this test is shown in Figure 3-4. The data show that addition of CAM and OTM improve hydrogen production. For the above tests, a CAM:OTM ratio of 4:1 resulted in maximum hydrogen production. The large amount of CAM resulted in a very low concentration of CO_2.

Future experiments will be performed at wider range of temperature and pressure to evaluate the effect of these variables on the overall process of hydrogen production via combined coal gasification and catalyst reactions.

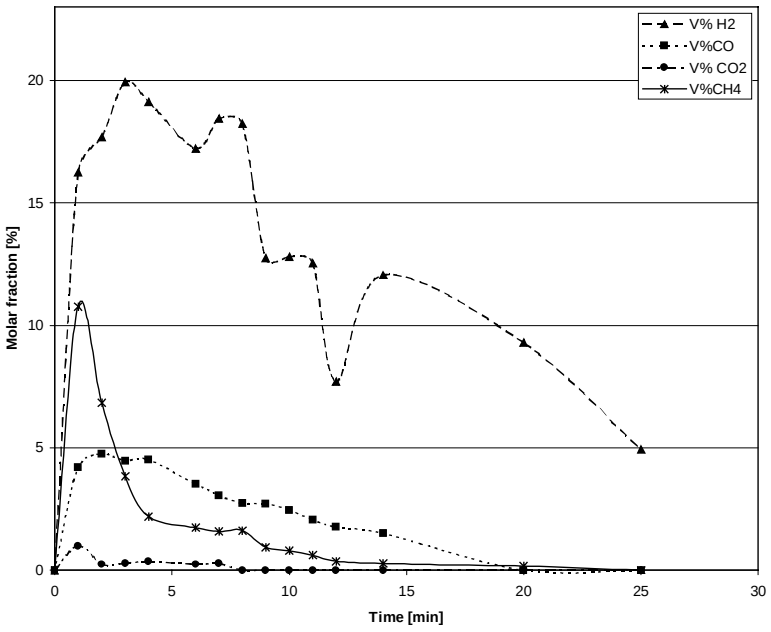

Figure 3-4. Test #38 product gas concentrations.

4.0 BENCH-SCALE TESTING (Task 3)

The objectives of the bench-scale testing task are to collect data on process operation and kinetics under dynamic fluidized bed conditions and aid in developing modeling tools and pilot plant equipment design. The bench-scale system is also intended to provide data on individual AGC processes to aid in pilot plant design and testing. Bench-scale testing conducted in the second program year has focused on performance assessments and parametric testing of the three key AGC processes: coal gasification (R1), CO_2 absorption (R1)/release (R2), and OTM oxidation (R3)/reduction (R2). In general, experimental results have served to illustrate the way the key processes occur, identify the key variables and ranges of operating conditions that produce the best results, and validate the overall AGC process by demonstration of its key reactions and processes.

4.1 Coal Gasification and CO_2 Absorption/Release (R1/R2) Testing

Initial bench-scale testing focused on coal gasification and CO_2 absorption using a CAM bed. Preliminary tests were conducted with an inert bed to provide a baseline for comparison with tests conducted with a CAM bed. A comparison is provided in Figure 4-1, which shows the total product gas flow rate for two coal gasification tests: inert bed and CAM bed. A significantly higher flow rate was produced for the inert bed case. Figure 4-2 further illustrates the distinction between these two tests via the contribution of CO_2 to the total flow rate. In Figure 4-2, the CO_2 present in the product gas is significantly lower, and is near zero at the beginning of the CAM bed test. The CO_2 concentration increases more rapidly and with a higher peak concentration during gasification in an inert bed. The CO concentration behaves in a similar manner, with increased concentrations during gasification in an inert bed. The reduced CO_2 concentrations are due to the absorption of CO_2 by the CAM bed. Meanwhile, the reduction in CO is caused by the participation of CO in the water-gas shift reaction ($CO + H_2O$ -» $CO_2 + H_2$), driven by the low CO_2 and CO concentrations in the reactor. A unique feature of the AGC process is its inherent production of high-purity H_2 due to the absorption of CO_2 and related reduction in CO concentration. Early experiments confirmed this capability.

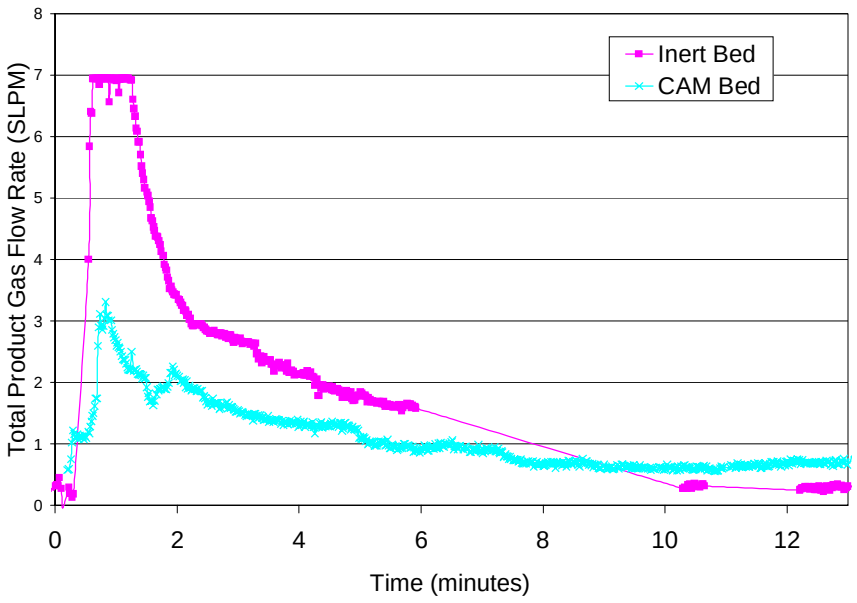

Figure 4-1. Total product gas flow rate during coal gasification tests conducted with inert bed and CAM (CO_2-absorbing material) bed.

Further investigation was directed at quantifying H_2 production and CO_2 absorption. As discussed above, the absorption of CO_2 during coal gasification has a significant impact on product gas composition. Unfortunately, CO_2 absorption cannot be measured directly; however, indirect measurements can be made of the CO_2 released during a subsequent regeneration step. The regeneration of CAM is conducted at an elevated temperature, generally 920°C. In previous tests conducted with an inert bed, all of the CO_2 generated was released during coal gasification. In contrast, using a bed composed of CAM, only a small fraction of the CO_2 is released during coal gasification; the remainder is absorbed by the CAM and released during a subsequent regeneration step. This process is depicted in Figure 4-3 for both an inert bed and a CAM bed. The CO_2 flow rate is significantly higher for the inert bed case during coal gasification, while for the CAM bed, the CO_2 flow rate reaches its peak value during the regeneration step after the CAM regeneration temperature is reached.

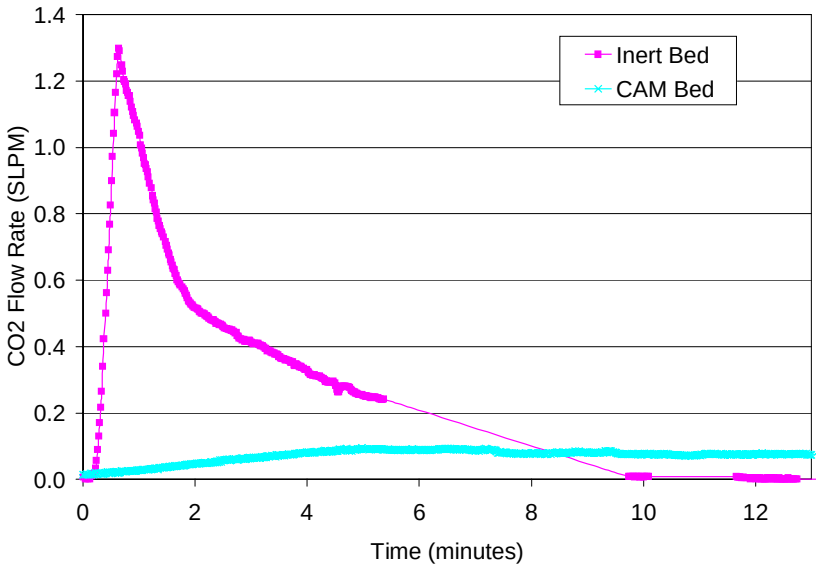

Figure 4-2. Flow rate of CO_2 in gasification product gas for tests conducted with inert bed and CAM (CO_2-absorbing material) bed.

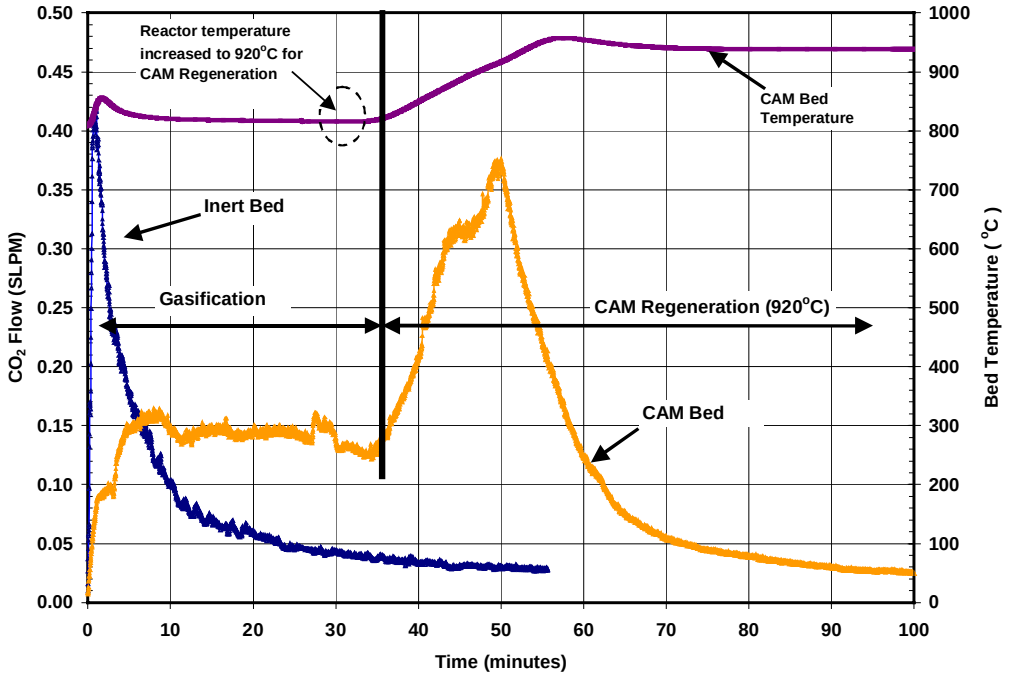

Figure 4-3. CO_2 release during coal gasification and CAM regeneration for a CAM bed, and during coal gasification for an inert bed. Temperature profile also shown for CAM bed case.

4.1.1 Parametric Testing: Impact of Gasification Temperature

Temperature is a key variable affecting CO_2 absorption and release. In order to quantify its impact, coal gasification experiments were conducted at temperatures of 750, 800 and 850°C, followed by CAM regeneration at 920°C. CO_2 concentrations from these tests are provided in Figure 4-4. Since the total amount of carbon present in the system is fixed, more CO_2 present during the coal gasification step leads to less CO_2 present during the CAM regeneration (CO_2 release) step. As might be expected, as the bed temperature approaches the CAM regeneration temperature, less CO_2 is absorbed. At higher temperatures, the equilibrium between CO_2 absorption and release is biased toward CO_2 release.

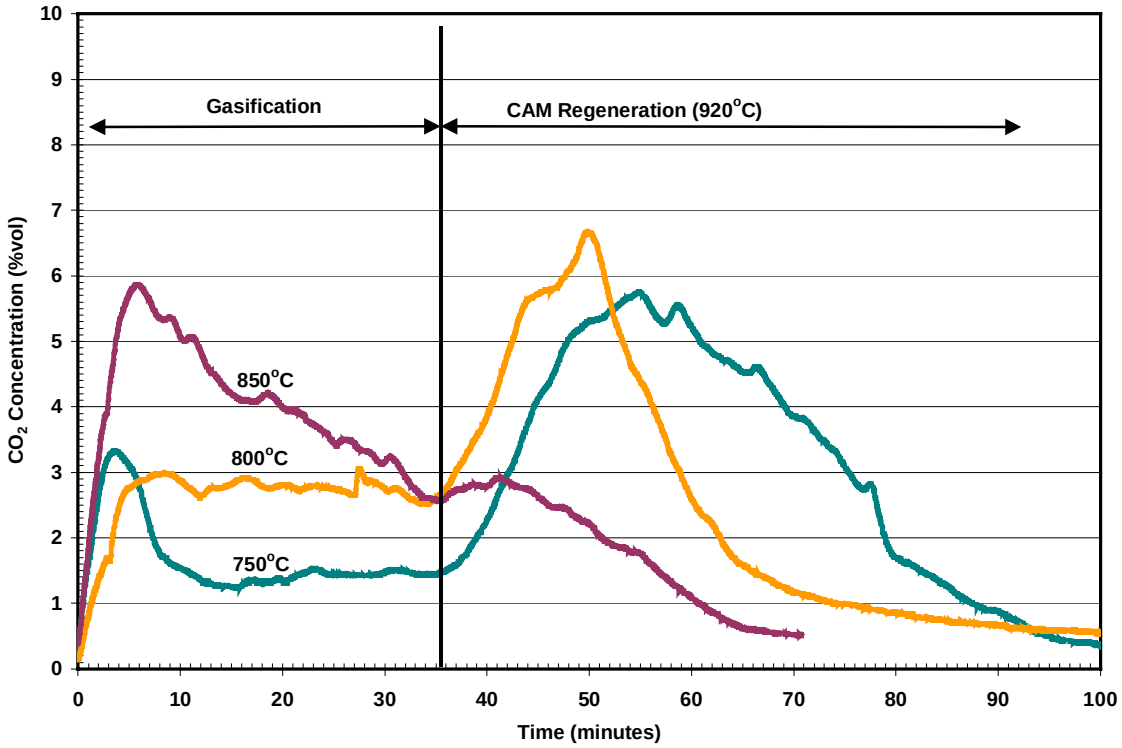

Figure 4-4. CO_2 concentrations at three different gasification temperatures, with CO_2 release at 920°C for each run.

Thus, at 850°C, the CO_2 concentration during coal gasification is significantly higher than at the lower temperatures. As a result of this reduced CO_2 absorption, less CO_2 is released during the CAM regeneration step. At both 750 and 800°C, peak CO_2 concentrations were achieved during the CAM regeneration step, indicating increased levels of CO_2 absorption during the coal gasification step.

However, CO_2 concentrations do not tell the whole story; the objective of the coal gasification step is to produce high-purity hydrogen. Figure 4-5 shows hydrogen concentrations at the three gasification temperatures. H_2 concentrations greater than 80% were achieved at 750 and 800°C. The increased CO_2 concentration present at 850°C has the effect of decreasing the H_2 concentration, peaking at only 72%. Although H_2 concentrations were similar at 750 and 800°C, the H_2 flow rates varied as indicated in Figure 4-6. H_2 flow rates are provided for the first 15

minutes of the 30-minute gasification step, as flows are relatively constant and very small after that time. Note that the majority of the flow occurs in the first five minutes of the step. The highest peak flow rate was achieved at 800°C, substantially higher than that achieved at 750°C, despite the similar product H_2 concentrations at these two temperatures. The H_2 flows at 850°C are less impressive when the low H_2 concentrations (and thus high impurity concentrations) are considered.

It is necessary to strike a balance between a bed temperature too high for CO_2 absorption to occur and a temperature so low that the coal gasification is hampered. Based on these bench-scale testing results, 800°C was selected as the optimal temperature for coal gasification tests.

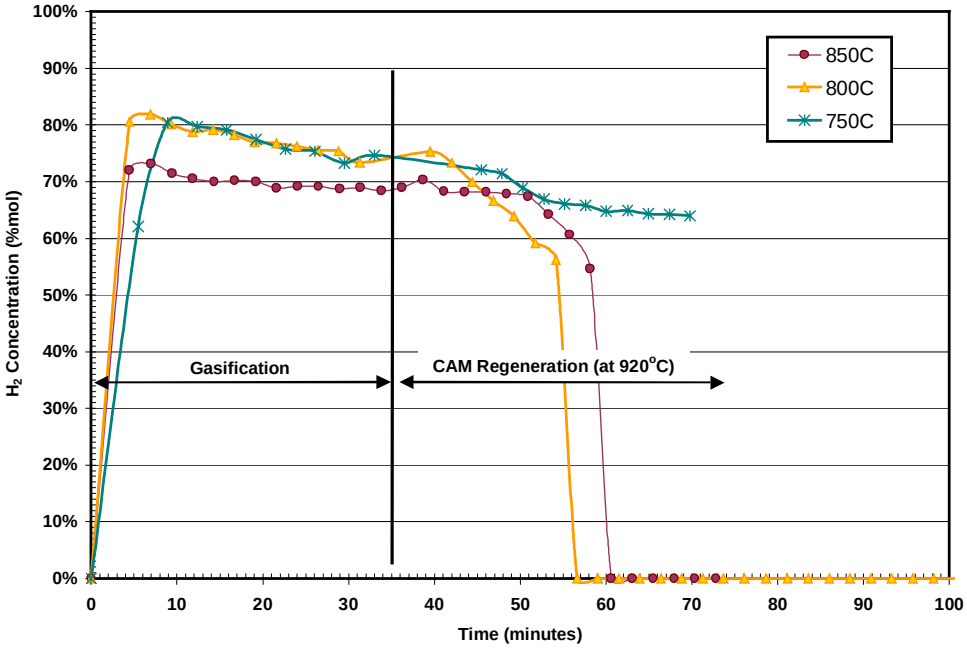

Figure 4-5. H_2 concentrations at three different bed temperatures during gasification and CAM regeneration.

The experimental investigation of coal gasification and CO_2 absorption provided quantitative data on the impact of R1 temperature on H_2 yield and purity as well as CAM effectiveness. This data has been used to identify desirable operating conditions and will be used to validate predicted behavior from process modeling efforts.

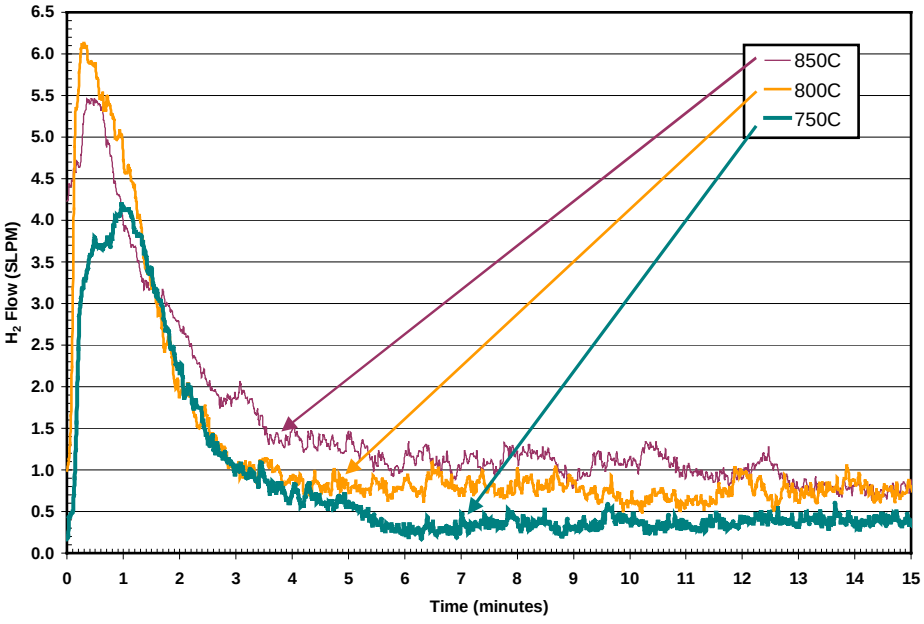

Figure 4-6. H_2 flow at three different bed temperatures during the gasification step.

4.2 Oxygen Transfer Material (R2/R3) Performance

OTM performance is related to the ability of the OTM to undergo the reduction reactions in Reactor 2 that in turn allow the OTM to be oxidized in Reactor 3. Experiments conducted under Reactor 3 conditions have shown that the oxidation of reduced-state OTM occurs rapidly and readily and is highly exothermic. OTM performance is most often limited by the reduction step. Initial OTM tests were conducted using coal for OTM reduction. Later tests were conducted using CO and H_2 as reducing agents to isolate OTM reduction from coal gasification. The complexity of the behavior observed led to the development of a designed experimental matrix involving the reduction of OTM with a range of concentrations of CO and/or H_2. These detailed experiments were conducted to further characterize OTM reduction behavior and establish kinetic rate constants for process modeling efforts.

4.2.1 OTM Reduction with Coal

OTM/coal tests were conducted in two steps. First, a 920ºC OTM bed was fluidized by steam, then a batch of coal was fed to the reactor. The coal gasification products (primarily CO and H_2) provide the fuel for OTM reduction. In the AGC process, the fuel for OTM reduction is char that is transferred from Reactor 1. However, as the objective of these initial tests was to verify that the OTM bed could undergo oxidation/reduction with gasified fuel, the use of coal in place of char has a minimal impact on the interpretation of results. Later tests will focus on char burnout levels required to provide sufficient fuel for OTM reduction once limits of OTM reduction are established.

The second step of the OTM test was OTM oxidation, accomplished by first lowering the temperature of the reactor to 750ºC under a nitrogen flow (to protect system components once the reactor temperature was elevated due to OTM oxidation), then feeding air to the reactor and measuring the temperature increase in the bed and the oxygen concentration of the product gas. Figure 4-7 shows the temperature profile during an OTM test. This figure indicates that the temperature increase during the oxidation step is rapid and significant. The magnitude of the temperature increase during the oxidation step is an indirect measure of the amount of OTM that was reduced (and thus made available for oxidation) in the reduction step. The amount of O_2 consumed may also be used as an indirect measure of the amount of OTM that was reduced during the reduction step.

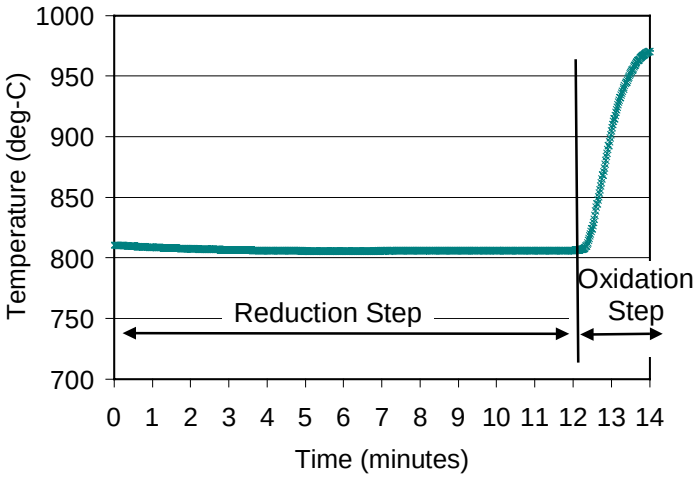

Figure 4-7. Temperature profile during reduction and oxidation steps of OTM test.

The extent of OTM reduction is related to the amount of reducing fuel present. During the OTM tests, varying amounts of coal were used to provide the fuel for OTM reduction. The objective of these tests was to identify maximum temperature increase achievable during the oxidation step.

During the OTM reduction step, CO_2 concentrations in the product gas are an indication of the extent of both coal gasification and OTM reduction, as CO_2 is a product of both of these processes. Figure 4-8 shows the measured CO_2 concentrations for tests conducted at three different coal:OTM ratios. It is interesting to note that the highest CO_2 concentrations were achieved during the 0.033 coal:OTM test, although this was not the highest fuel input tested.

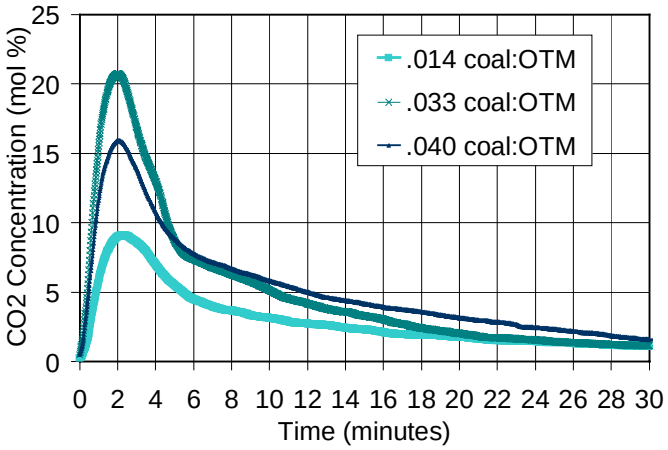

Figure 4-8. CO_2 concentrations during the reduction step of OTM tests for three different coal:OTM ratios.

However, temperature increases measured during the oxidation step of the OTM tests are consistent with the CO_2 concentration results, as the 0.033 coal:OTM ratio test also produced the largest temperature increase (Figure 4-8). Preliminary results in this figure suggest that excess fuel may adversely impact the OTM oxidation/reduction cycle, as can insufficient fuel. The test with the highest coal:OTM ratio (0.040) produced a significantly lower temperature increase than the two tests with lower fuel inputs. Further investigation is currently in progress to look into the reproducibility of this data and provide more information on the mechanism by which increased fuel decreases the ability of the OTM to be reduced and oxidized, as well as exploring the limiting value of the fuel input required to promote optimized OTM oxidation/reduction.

4.2.2 OTM Reduction with CO and H_2 (Fluidization Medium: N_2)

As part of this effort, another set of experiments was conducted to separately identify the extent of OTM oxidation by CO and H_2. In these tests, coal was replaced with gas mixtures of either CO or H_2 (balance N_2) to simulate simplified Reactor 2 OTM reduction conditions. A sample of experimental results is provided in Figure 4-9, which shows the outlet H_2 concentration during two tests of OTM reduction performed at different H_2 feed concentrations. As may be expected, the H_2 concentration more quickly reaches its inlet concentration for the 20% H_2 case, while the 6% H_2 case approached the inlet concentration more gradually.

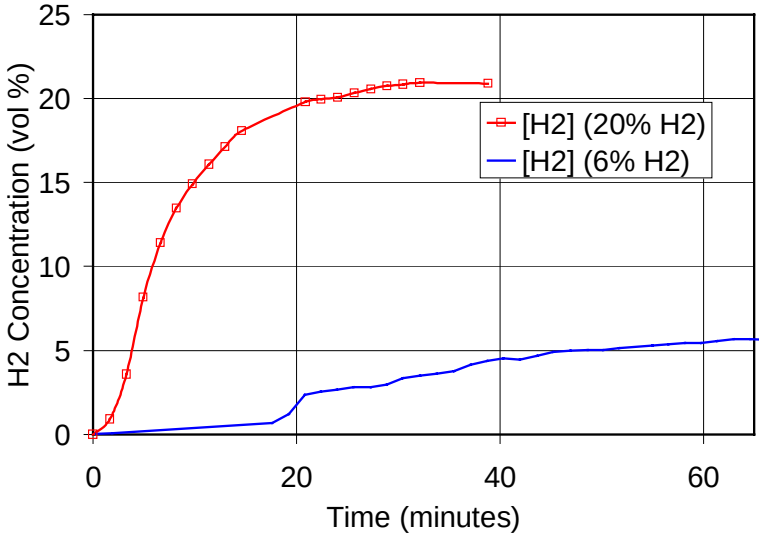

Figure 4-9. H_2 concentration during OTM reduction step for two different H_2 feed concentrations.

However, during the oxidation step that followed these OTM reduction steps, the 6% H_2 case experienced a significantly larger temperature increase, as shown in Figure 4-10. The temperature increase was so large, it was necessary to reduce the air feed flow rate to prevent equipment damage. After the system temperature decreased, the airflow rate was increased, causing another temperature spike that required a subsequent airflow reduction. The airflow rate was later increased again to its original level. The temperature increase for the 20% H_2 case was much more gradual and had a lower maximum. Initially, it was thought that the extent of OTM reduction might be more complete for the higher H_2 feed concentration and lead to a larger temperature increase, but this was not supported by experimental results. Obviously, the concentration of the reducing fuel (here H_2) plays an important role in the extent of OTM reduction. This role is being explored further in a set of designed experiments, described below.

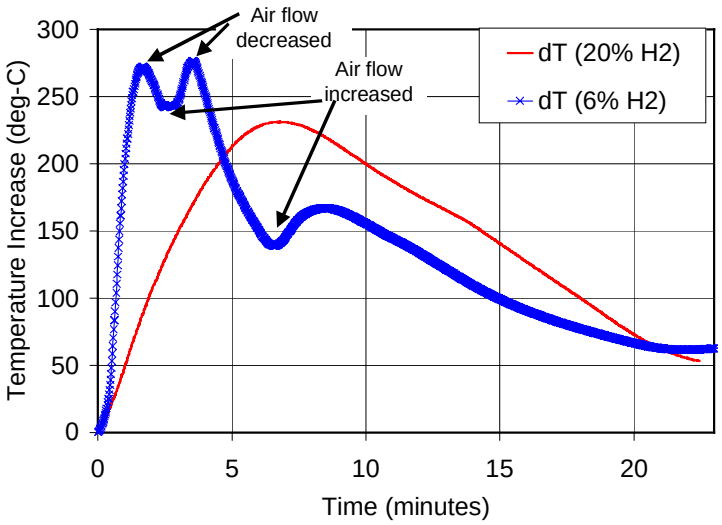

Figure 4-10. Temperature increase during OTM oxidation step for two different H_2 concentration

4.2.3 OTM Reduction with CO and H_2 (Fluidization Medium: Steam)

Continuing investigations are in progress to further characterize OTM behavior relative to the CO and H_2 reducing agents at various concentrations/mixtures. A test matrix, provided as Table 4-1, was developed to provide quantitative information on the relationships between reactant concentrations, OTM reduction, and OTM oxidation. The test matrix will facilitate the collection of data that can be analyzed using statistical methods to determine the response surface of OTM reduction performance. The required experiments are still in progress, and are expected to be complete in the next quarter. Preliminary results provide insight into the behavior of interest.

Table 4-1. Test matrix for OTM reduction/oxidation experiments.

Test Conditions				
Run #	CO Feed (L/min)	H_2 Feed (L/min)	OTM (grams)	Duration (hours)
1	0.5	2	200	5
2	1	1	250	5
3	0	1	200	5
4	1	2	250	5
5	1	0	200	5
6	0	2	150	5
7	0	2	250	5
8	1	0	150	5
9	0.5	1	200	5
10	0.5	0	250	5
11	0	0	150	5
12	1	2	150	5
13	0.5	1	150	5
Validation Test Conditions				
1v	0.5	0.5	219.5	5
2v	0.2	0.4	233.7	5
3v	0.5	0.8	234.6	5

Analysis of OTM performance is complicated by the participation of the OTM reduction reactants and products in the water-gas shift reaction when CO is one of the reactants. The key reactions are shown below. The water-gas shift reaction is reversible and highly dependent on local

concentrations. Thus, composition measurements of the product gas must be interpreted with care, as reduction products can, in turn, become water-gas shift reactants. In the AGC process, both CO and H_2 are produced by coal gasification/char oxidation in Reactor 2, while steam is fed as the fluidizing gas. However, the complexity of these interactions provides limited data concerning the individual kinetic rates of CO and H_2 consumption by OTM reduction.

OTM-O + CO -> 2OTM + $CO_{2\text{-red}}$	OTM reduction with CO
OTM-O + H_2 -> 2OTM + H_2O	OTM reduction with H_2
CO +H_2O -> CO_2^* + H_2	water-gas shift

Where, OTM-O is the oxidized state of OTM.

The distinction between the OTM reduction reactions and the water-gas shift reactions is most clear in tests using CO as the reducing gas. CO_2 is a product of both the OTM reduction and the water-gas shift reactions. Since H_2 is not a product of the OTM reduction reactions, the amount of H_2 in the product gas is an indication of the extent of the water-gas shift reaction (and thus the amount of CO_2 produced via the water-gas shift reaction). Thus $\{H_2\} = \{CO_2^*\}$, where $\{H_2\}$ is the number of moles of H_2 and $\{CO_2^*\}$ is the number of moles of CO_2 produced via the water-gas shift reaction. Using {} in the text below symbolizes number of moles of the chemical constituent between the brackets.

The measured CO_2 concentration is composed of contributions from both the water-gas shift and the OTM reduction reactions; thus, for tests of reduction by CO, $\{CO_{2\text{-tot}}\} = \{CO_{2\text{-red}}\} + \{CO_2^*\}$ and $\{CO_{2\text{-red}}\} = \{CO_{2\text{-tot}}\} - \{CO_2^*\}$. The degree of OTM reduction can be determined by relating $\{CO_{2\text{-red}}\}$ to the OTM-O concentration and comparing this value to the initial amount of OTM-O in the bed $\{\text{OTM-O}_{bed}\}$ per the OTM reduction with CO reaction above. Thus, since the stoichiometry of the reduction reaction with CO dictates that one mole of CO_2 is produced for every mole of OTM-O (i.e., $\{CO_{2\text{-red}}\} = \{\text{OTM-O}\}$), %OTM reduction = $\{CO_{2\text{-red}}\}$ / $\{\text{OTM-O}_{bed}\}$. This can be easily calculated since $\{CO_{2\text{-red}}\}$ can be obtained from the measured $CO_{2\text{-red}}$ concentration and the $\{\text{OTM-O}_{bed}\}$ can be obtained from the weighted OTM-O_{bed} initial amount.

The oxidation step (simulating Reactor 3 in the AGC process) involves the reaction:

OTM + ½ O_2 -> OTM-O

The measured amount of O_2 consumed can also be used to independently arrive at a % OTM reduction level. Since ½ mole of O_2 reacts to produce each mole of OTM-O, $\{\text{OTM-O}_{oxid}\} = ½ \{O_2\}$, where $\{O_2\}$ is the number of moles of O_2 consumed. Thus, %OTM reduction = ½ $\{O_2\}$ / $\{\text{OTM-O}_{bed}\}$.

In test matrix runs #5 and #10, CO was used as the sole reducing gas. For these tests, the %OTM reduction was calculated by the two above-described methods: CO_2 generated (based on measurements of CO_2 taken during the reduction step) and oxygen consumed (based on measurements of O_2 taken during the oxidation step). Table 4-2 shows a reasonably good agreement between results calculated via the two methods; for Run #5, 10.4 vs. 9.5% OTM reduction, and for Run #10, 12.5 vs. 12.8% OTM reduction. The good agreement between these values provides support for the calculation assumptions, especially relative to the amount of

CO_2* from the water-gas shift reaction. It is worth mentioning here that based on these two runs with CO, the OTM:%CO ratio that would provide the optimum reduction has not been found yet since as the ratio increased the reduction also increased (Table 4-2). Future experiments have been designed to increase the ratio further to identify the optimum reduction.

Table 4-2. Results of CO reduction experiments: %OTM reduction calculated via both reduction step and oxidation step experimental measurements.

run #	mol OTM in bed	Reduction Step				Oxidation Step		
		OTM : %CO ratio	% CO fed	mol CO_2 generated by OTM reduction	**% OTM reduction—Reduction Step**	% O_2 fed	mol O_2 consumed	**% OTM reduction—Oxidation Step**
5	1.28	0.16	8	0.13	**10.4**	4.1	0.24	**9.5**
10	1.57	0.39	4	0.20	**12.5**	7.4	0.40	**12.8**

Figure 4-11 illustrates the molar flow rates of CO, CO_2 and H_2 during Run #5, an OTM reduction test with CO. The flow rate of CO_2 increased immediately at the start of the test, while there was an approximately 3-minute time lag before the H_2 flow increased. This suggests that the initial CO_2 increase was due to the OTM reduction reaction and that this reaction is dominant at the beginning. As the test proceeded, however, the water-gas shift reaction began to dominate evident by the increased H_2 production. This experimental data lends further support to the assumptions made for data reduction.

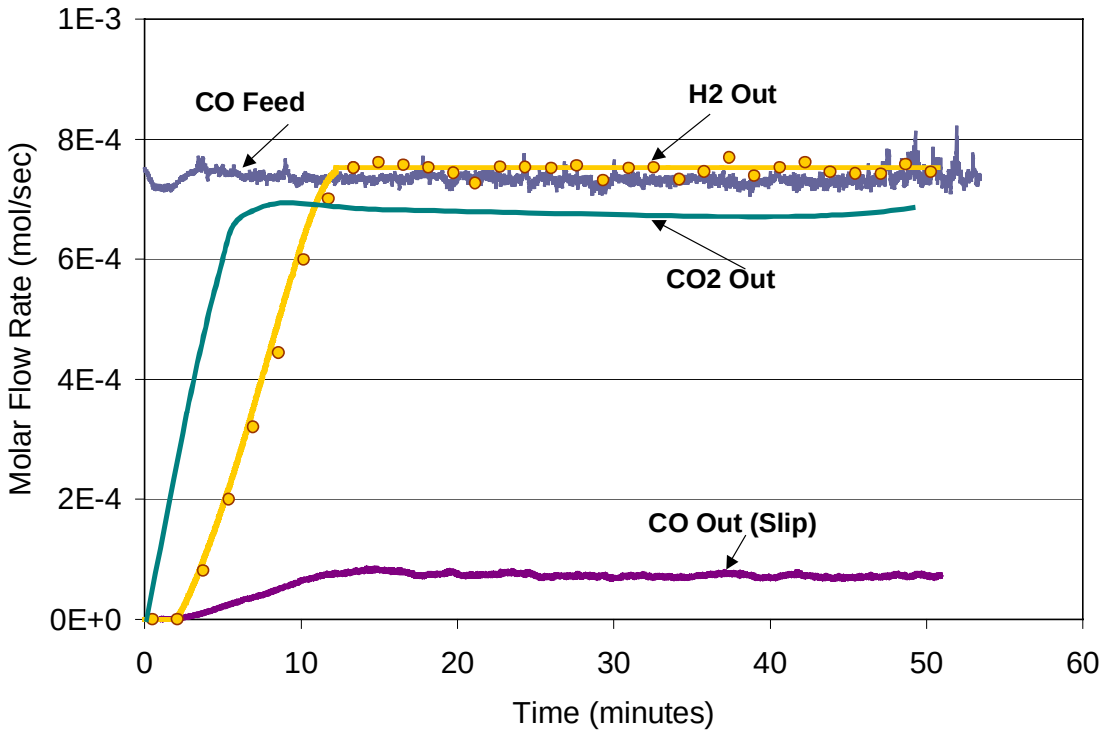

Figure 4-11. OTM reduction by CO: production of CO_2 and H_2 (Run #5).

Other preliminary test results show that the test matrix is in the appropriate design space to identify optimized conditions for OTM reduction. Figure 4-12 shows the % OTM reduction achieved at a variety of ratios of moles of OTM to %H_2 fed. These results indicate that increasing the OTM:H_2 ratio does not steadily increase OTM reduction; the highest ratio (0.18) shows markedly lower OTM oxidation than the 0.12 ratio test, which provided the optimum reduction when H_2 was used as the reducing agent.

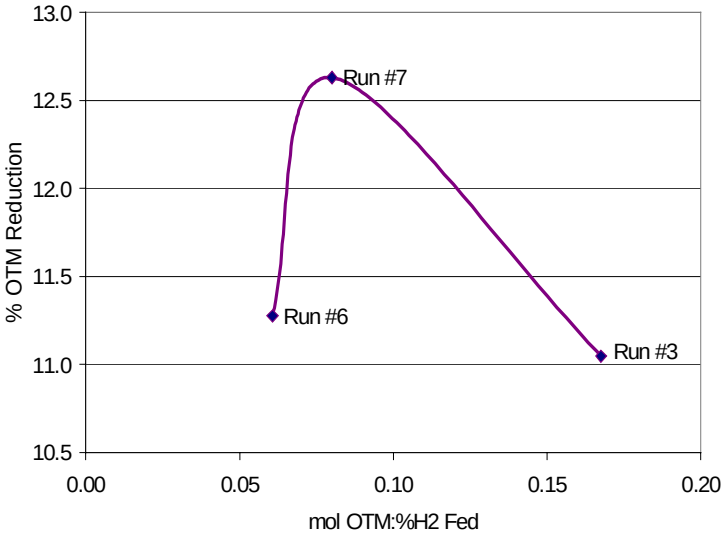

Figure 4-12. %OTM reduction as a function of the ratio of OTM moles:% H2 fed.

An oxidation step was conducted after each OTM reduction step. Based on the comparison of the results of %OTM reduction for the CO reduction cases described above, O_2 consumption provides an accurate, though indirect, measure of OTM reduction. For the tests shown in Figure 4-13, the % O_2 fed was varied, which affected the initial oxygen consumption rate. However, the total O_2 consumed, depicted by the area under each curve (Figure 4-13) and shown in Table 4-3, was primarily influenced by the previous OTM reduction step. Additional testing is planned to identify modes for increasing OTM reduction performance.

Table 4-3. %OTM Reduction based on O_2 Consumption

run #	mol OTM:% H2 ratio	% OTM reduction
3	0.18	11.0
4	0.08	6.0
5	0.16	10.2
6	0.06	11.3
7	0.12	12.6
10	0.40	12.9

Analysis of experimental test matrix results is in progress and will be completed once the final test runs are conducted, in the next quarter. The statistical analysis of the complete experimental matrix will provide detailed quantitative performance information as well as provide insight into the OTM performance response surface. The next set of experiments will focus on OTM reduction by char, which will generate CO and H_2 simultaneously.

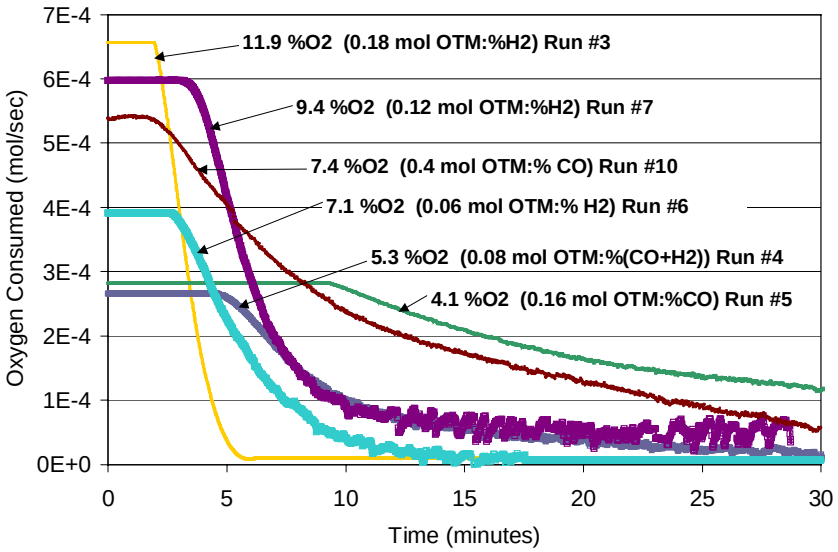

Figure 4-13. O_2 consumption during OTM air regeneration step.

5.0 ENGINEERING AND MODELING STUDIES (Task 4)

5.1 Preliminary Economic Assessment

The objective of the preliminary economic assessment is to establish target investment values that provide competitive costs of electricity (COE) and other co-products for coal/biomass power generation in order to compare the AGC system with other coal/biomass to electricity technologies. As part of this effort, a comparison between AGC and IGCC systems was developed to clearly identify key technical and other differences. A summary of the comparison is provided in Table 5-1. Although both IGCC and AGC systems produce electricity in a gas turbine, the AGC system also produces high-purity H_2 and reduces the need for air pollution control devices such as those required in the IGCC syngas cleanup step. In addition, the AGC process does not require a costly oxygen plant. The IGCC technology has been demonstrated at large scales at different locations in the world and thus the economics of IGCC plants are well characterized and will be used as a target for AGC costs.

Table 5-1. Comparison of features of AGC technology and IGCC (Integrated gasification combined cycle) technology.

Feature	AGC	IGCC
Major components	Steam gasification (Reactor 1)	Gasification (with air or O_2)
	CO_2, sulfur sequestration (Reactor 2)	Syngas cleanup
	Metal oxidation/heat generation (Reactor 3)	
	Gas turbine combined cycle	Gas turbine combined cycle
		Oxygen plant
Product streams	High-purity hydrogen stream (>90%)	Syngas
	Sequestration-ready CO_2 stream containing sulfur and other pollutants	Syngas cleanup products (potential for marketable products)
	Power from gas turbine	Power from gas turbine
Intermediate streams		Syngas (8.6-61% H_2),
	High-pressure air	High-pressure syngas
	High-pressure, high-temperature feed for gas turbine	High-pressure feed for gas turbine
Pollutants	Minimal cleanup of H_2-rich fuel required for fuel cell operation (majority of pollutants concentrated in CO_2 stream)	Sulfur removal is required
	No NO_x formation	Gas turbine optimized to minimize NOx formation
	Hg concentrated in Reactor 1 product stream	Hg concentrated in syngas stream
Gas turbine operation	N_2-rich stream expanded in gas turbine	Syngas combusted in gas turbine
Fuel flexibility	Coal, biomass planned	Demonstrated use of coal, coke, biomass, waste
Economics	TBD	Turnkey cost (coal fuel) $1,000-$1250/kW

A preliminary estimate of the costs of electricity and hydrogen was conducted for the AGC system. The estimate was made using established cost estimation methodologies, as was detailed in Appendix A of the April 2002 Quarterly Technical Progress Report. Some of the key assumptions made for the AGC base case are provided in Table 5-2. Using the cost estimation methodology established previously for estimating capital and operating costs, the cost of electricity was calculated for the AGC system. A mass and energy balance was prepared to provide the basis for fuel and materials costs. Standard assumptions for capital costs were made including cost estimates for the major system components. Operating, maintenance and labor costs were estimated using empirical correlations with total capital requirement costs. Estimates of fuel costs, capacity factors, hybrid fuel cell efficiency and hybrid fuel cell costs were the subject of a sensitivity analysis to identify the impact of varying assumptions on the cost of electricity. The results of the sensitivity analysis were also provided in Appendix A of April 2002 Quarterly Technical Progress Report.

Table 5-2. Key assumptions for the preliminary economic evaluation.

Coal capacity	2800 t/day
Capital recovery factor	15%
Fuel cost	$1.25/MMBtu
Plant capacity factor	75%
Hybrid fuel cell efficiency	75%
Hybrid fuel cell capital cost	$500/kW
O&M Cost (excluding fuel)	4% of capital cost
Capital Cost	$1500/kW

A review of the literature on IGCC costs identified several recent studies of IGCC costs, both with and without add-on CO_2 sequestration equipment. The AGC system, which provides inherent CO_2 capture, has costs that compare favorably with IGCC costs, as shown in Table 5-3. The AGC costs were developed from the preliminary economic evaluation detailed in Appendix A of the April 2002 Quarterly Technical Progress Report. AGC costs were comparable with those of IGCC, and superior to IGCC with CO_2 capture.

The economics of the AGC process are critical to its eventual commercialization. Developing relationships between technical performance goals and economic targets will ensure that AGC development results in a viable commercial product.

Table 5-3. Comparison of cost of electricity for IGCC and AGC systems.

System Type:		IGCC w/o CO_2 capture			IGCC w/ CO_2 capture		AGC
Basis		Avg of many studies*	Destec**	Texaco***	Avg of many studies*	Destec w/ Selexol**	Preliminary Economic Evaluation
Plant Size	MW	400	400	400	400	400	400
Fuel Cost	$/MMBtu	1.24	1.24	1.24	1.24	1.24	1.24
Capacity factor	%	75	65	85	75	65	75
CO_2 Capture	%	0	0	0	90	90	99
Capital Recovery Factor	%	0.15	0.16	0.18	0.15	0.16	0.15
Efficiency	% (LHV)	42.2	44.7	48.3	36.1	38.4	57.4
Capital Cost	$/kW	1401	1260	1370	1909	1642	1605
Cost of Electricity							
Levelized Capital	$/kWh	0.032	0.035	0.033	0.044	0.045	0.037
O&M	$/kWh	0.008	0.008	0.006	0.012	0.010	0.010
Fuel	$/kWh	0.010	0.010	0.010	0.012	0.011	0.006
Total COE	**$/kWh**	**0.050**	**0.052**	**0.049**	**0.067**	**0.066**	**0.053**

Costs includes: delivery, material, installation, labor, engineering, contingency

* David, J. and H. Herzog, "The Cost of Carbon Capture," Presented at DOE NETL First Annual Conference on Carbon Sequestration, May 2001, Washington, DC

** EPRI, Evaluation of Innovative Fossil Fuel Plants with CO_2 Removal, Dec 2000.

*** DOE NETL Process Engineering Division, Texaco Gasifier IGCC Base Cases, PED-IGCC-98-001, June 2000 rev.

5.2 Process Modeling

A steady state process analysis model has been developed to integrate the three AGC reactors, predicting temperatures and product compositions, as part of the AGC plant heat and mass balance. The program is linked with the FORTRAN-based NASA Chemical Equilibrium code and assumes that equilibrium is reached under adiabatic conditions at the exit temperatures, thus predicting compositions and temperatures by trial and error.

As previously described in the Appendix B of the April 2002 Quarterly Technical Progress Report, a new generic heat transfer model was developed for a fluidized bed. From the dimensions of the bed, the reactant and product compositions and the reactant inlet temperatures, the model determines the outlet temperature, inside and outside wall temperatures and heat losses. The model can be used for any of the three Vision 21 reactors, operating in either the bubbling fluidization regime or the fast fluidization regime.

An integrated model is being developed to predict fluidization characteristics and heat losses, coupling them to the chemistry (product distribution) to aid in evaluation of the cold flow model of the pilot-scale system. This new tool will be used for design optimization, as well as pilot-scale data analysis and validation.

The FORTRAN-based current process analysis model has convergence problems and is not robust to be effectively integrated with the heat transfer model. Calling FORTRAN subroutines to recalculate the new equilibrium compositions every time the process inputs are changed is time consuming and does not always lead to valid results because the subroutines sometimes do not converge. New tools have been identified to aid in the effective integration of the process model with the heat transfer model. To this end, two new software tools have been obtained for process modeling:

- The HSC Chemistry™ 5.0 chemical reaction and equilibrium software. Given the temperature and pressure conditions, HSC calculates the equilibrium compositions of species. The output can be stored in Excel format as lookup tables.
- The ASPEN™ Process Engineering software, a fully functional process design program.

Continuing modeling work will make use of HSC Chemistry™ and ASPEN™ to assess several equilibrium cases and quantify the relationships between basic input parameters for the Vision 21 reactors (Steam to carbon ratio, Fe/Ca ratio, temperature, pressure etc) and performance. Continuous transfer functions for calculating the product compositions will be developed and coupled with the heat transfer model. The transfer functions will also account for non-idealities of the equilibrium, assuming a conversion or temperature approach for some reactions, particularly the CO_2 absorption by CAM.

The DFSS (Design for Six Sigma) methodology will be used to develop and validate the transfer functions. Statistical analysis using Minitab™ software will be conducted.

6.0 PILOT PLANT DESIGN AND ENGINEERING (Task 5)

Specific objectives of the pilot plant design effort include:

- Creation of a conceptual design for an AGC pilot-scale plant;
- Documentation of the process and instrumentation diagram (P&ID);
- Development of reactor designs for (1) fluidized gasification of coal/CO_2 absorption (Reactor 1), (2) CAM decomposition and OTM reduction (Reactor 2) and (3) OTM oxidation (Reactor 3); and
- Identification and specification of subsystems.

During the second program year, the design and engineering task was completed, and work began on pilot plant assembly (Task 6).

6.1 System Operating Conditions

The heart of the AGC process is the three fluidized bed reactors. Two types of criteria were used to determine the operating conditions of the three reactors: fluid dynamics (or fluidization) and chemistry (or stoichiometry). These two criteria defined the fluidization flow and the mass of bed material from AGC process requirements. It was important to identify operating conditions that met both criteria. An Excel spreadsheet was developed to utilize fluidization correlations from literature[1] and match them as closely as possible to the chemistry requirements.

Several situations with different reactor diameters and particle sizes were assessed. From this sensitivity analysis, a range of practical operating conditions and reactor specifications was obtained. A summary of this analysis is provided in Table 6-1. Operating limits for main process variables are shown.

Table 6-1. Pilot-scale operating conditions for AGC reactors 1-3.

Reactor	ID (in)	L_{mf} (ft)	Bed mass (lb)	Bed composition	L (ft)		L_{total} (ft)	$d_{p.avg}$ (μm)	coal feed (lb/h)	Steam flow (lb/h)	
					min	max				min	max
										183.8	320.8
										Steam-to-Carbon	
										min	max
										3.5	6
1	10	1.52	115.6	55% CAM 45% OTM	1.76	2.05	7.72	300	50 (max. 100)	Re	
										min	max
										4.01	7
										u/u_{mf}	
										min	max
										2	3.49

Reactor	ID (in)	L_{mf} (ft)	Bed mass (lb)	Bed composition	L (ft)		L_{total} (ft)	$d_{p.avg}$ (μm)	coal feed (lb/h)	Steam flow (lb/h)	
					min	max				min	max
										154.9	270.4
										Steam-to-Carbon	
										min	max
										5.22	9.11
2	10	1.52	115.6	35.75% CAM 64.25% OTM	1.76	2.05	7.72	300	N/A	Re	
										min	max
										4.01	7
										u/u_{mf}	
										min	max
										2	3.49

Reactor	ID (in)	L_{mf} (ft)	Bed mass (lb)	Bed composition	L (ft)		L_{total} (ft)	$d_{p.avg}$ (μm)	coal feed (lb/h)	Air flow (lb/h)	
					min	max				min	max
										177.6	378.2
										O_2/Fe	
										min	max
										0.098	0.209
3	10	1.49	113.8	55% CAM 45% OTM	1.74	2.16	5.28	300	N/A	Re	
										min	max
										2.93	6.25
										u/u_{mf}	
										min	max
										2	4.26

* L_{mf} is the length of bed at minimum fluidization (approx. the length of static bed), and L is the length of fluidized bed.

[1] Octave Levenspiel and Daizo Kunii, *Fluidization Engineering*, 2nd edition, Butterworth-Heinemann, 1991.

The minimum and maximum operating limits have set according to the minimum practical limit of fluidized bed operation and to the maximum condition before bed slugging occurs. Under these conditions, these fluidized beds will operate in the bubbling bed regime. The dimensions of each of the three reactors have been set at 8 feet in length with 10-inch inside diameters.

6.2 Reactor Heat Loss and Mechanical Stress Analysis

The harsh environment experienced by the AGC reactors required a detailed analysis of heat transfer and mechanical stress to ensure the integrity of the reactors and minimize the potential for material failure. The three reactors were designed for 300-psi pressure, while the reaction temperature may vary from 750 to 1300°C to accommodate the range of reactor temperatures. The upper temperature limit may potentially be achieved in Reactor 3, although Reactors 1 and 2 will typically have lower operating temperatures. However, all three reactors were designed to meet the same specifications. Key features of the reactor design are provided below:

- Metal shell material: 304 SS, schedule 40, 18" nominal OD
- Maximum shell temperature: 1000°F (538°C)
- Insulating liners (inside metal shell)
    - Innermost layer: high strength and abrasion resistance material
    - Outer layer: insulating, low thermal conductivity material
- Insulation (outside metal shell)
    - Minimal insulation to prevent excessive shell temperature

The design of the insulating liners figured prominently in the reactor design. Figure 6-1 depicts the different insulation layers. The innermost layer in Figure 6-1 is composed of high abrasive resistance material; a high-strength ceramic. The next layer is an insulating, low thermal conductivity material that will protect the metal shell from exposure to elevated temperatures. The third layer is the metal shell, which is rated for the operating pressure and shell temperature. The outermost layer is an insulating blanket, which will limit heat loss while also preventing excessive shell temperatures.

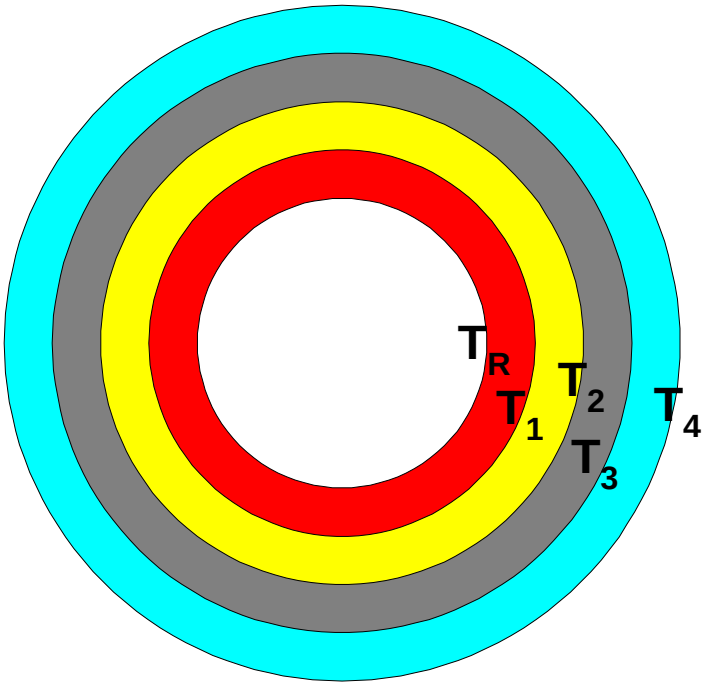

Figure 6-1. Cross-section of reactor insulation layers.

In Figure 6-1, T_R is the reaction temperature, while T_1, T_2 and T_3 are the temperatures at the boundaries, and T_4 is the desired temperature at the external surface of the insulating blanket. Calculating these temperatures for a given T_R is a problem of compounded thermal resistances, solved by calculating the sum of the thermal resistances of each layer, and assuming that the

temperature profile across each layer is proportional to the overall temperature profile from the innermost to the outermost layer. This calculation method was programmed in Excel to calculate the temperature at each boundary after a series of iterations. The overall heat loss is based on the thickness and material properties of each layer. A database of materials (ceramic, insulator and metal alloys) was assembled in the spreadsheet. The inside metal shell temperature (T_2) was used to calculate the safety factor based on the ASME code's maximum allowable mechanical stress.

The program is capable of handling up to three layers before the metal shell layer. The results of the calculations shown in Table 6-2 are the temperatures at each boundary, shown on the right side of Table 6-2. The predicted metal shell temperature is 487°C, providing a safety factor of 8.5. The maximum shell temperature (safety factor of one) is 712°C. The materials selected for use in the reactors include:

1st layer (innermost): KAO-TAB 95 (from Thermal Ceramics).
2nd layer: KAOLITE 2300-LI (from Thermal Ceramics).
3rd layer: SS304L-Schedule 40, 18 inch nominal ID.
4th layer (outermost): KAOWOOL #8.

Table 6-2. Template for calculating temperature profile across reactor and insulation layers.

THIS SPREADSHEET CALCULATES THE Q_{lost} PREDICTED AND THE TEMPERATURE PROFILE ACROSS THE LAYERS

Reactor	ΔH (kcal/s)	T_r (°C)	T_r (°F)
1	65900	1000	1832
2	133325	1000	1832
3	158328	1300	2372

Choose Reactor: 3

Choose ID_{liner} (in):	10
Choose $t_{liner\ 1}$ (in):	1.000
Choose $t_{liner\ 2}$ (in):	2.500
Choose $t_{liner\ 3}$ (in):	0.000
Choose t_{shell} (in):	0.562
Choose t_{ins} (in):	0.500
Choose clearance (in):	0
Length of cylinder (in):	96
(m):	2.44

		Temp. (°C)		$\Delta T_{approach}$ (°C)
T_{in} (°C) =	1300.0			
T_{out} (°C) =	25.0	hot face	cold face	
$k_{liner\ 1}$ (W/m.K) =	1.70	1300	1246	1.0E-04
$k_{liner\ 2}$ (W/m.K) =	0.23	1246	488	2.6E-07
$k_{liner\ 3}$ (W/m.K) =	0.19	488	488	1.4E-04
k_{shell} (W/m.K) =	21.27	488	487	5.2E-04
k_{ins} (W/m.K) =	0.06	487	43	2.5E-06
h_{out} (W/m^2.K) =	3.00			

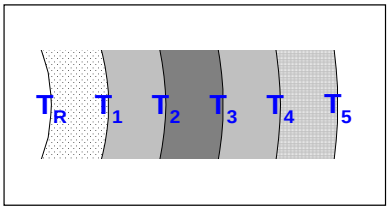

Boundary Temperatures

	OD (in)	ID (in)	t (in)
Liner 1	12.00	10.00	1.00
Liner 2	17.00	12.00	2.50
Liner 3	17.00	17.00	0.00
Shell	18.12	17.00	0.562
Insulation	19.12	18.12	0.50

Q_{lost} (W) =	7773

No.	Layer	R (K/W)	T (°C)	T (°F)
1	Reaction		1300	2372
2	Liner 1	0.0070	1246	2274
3	Liner 2	0.0974	488	911
4	Liner 3	0.0000	488	911
5	Shell	0.0002	487	908
6	Insulation	0.0571	43	109
	Environ.	0.0023	25	77
	Total	0.1640		

Shell stress S.F. (mechanical):	8.53
Maximum temp. to expose shell (°C):	712

The inner ceramic layers will be cast and cured inside the metal shell at GE EER's test site. The use of castable insulation will prevent the presence of air gaps between layers.

The heat loss and mechanical stress analysis confirms that the design of the AGC reactor meets the process specifications and can withstand the harsh conditions of the AGC process.

6.3 Solids Transfer Mechanism

The transfer of solid bed materials between reactors is a critical part of the AGC process, as it serves to transfer heat and regenerated reactants between reactors. A full-size pilot-scale cold flow model was constructed to simulate the action of the solids transfer ducts. Figure 6-2 is a photograph of the cold flow model, built with transparent plexiglass with transfer ducts. The cold flow model was initially constructed with two reactors. Future testing will integrate the third reactor after reasonable solids transfer operating parameters have been established.

Figure 6-2. Cold-flow model of pilot-scale solids transfer system (2-reactor version).

The first objective of the cold flow simulation was to study the parameters that influence solids transfer and prevent or minimize solids accumulation, clogging and heat loss during transport. The second important objective is to minimize the auxiliary steam flow (solids carrier gas flow) required for solids transport.

Several solids transport modes have been identified and compared. An initial method assumed that solids should move from the top of one fluidized bed to the bottom of the next. However, early experiments demonstrated that this method is not feasible in practice; the head pressure at the intake point is lower than the head pressure at the delivery point, requiring excessive solids

carrier gas flows to ensure transport. The direction of solids flow was subsequently reversed, allowing solids transfer with reasonably small flow rates of auxiliary carrier gas (25-50% of the fluidization gas flow rate). A simplified schematic of the AGC system showing the direction of

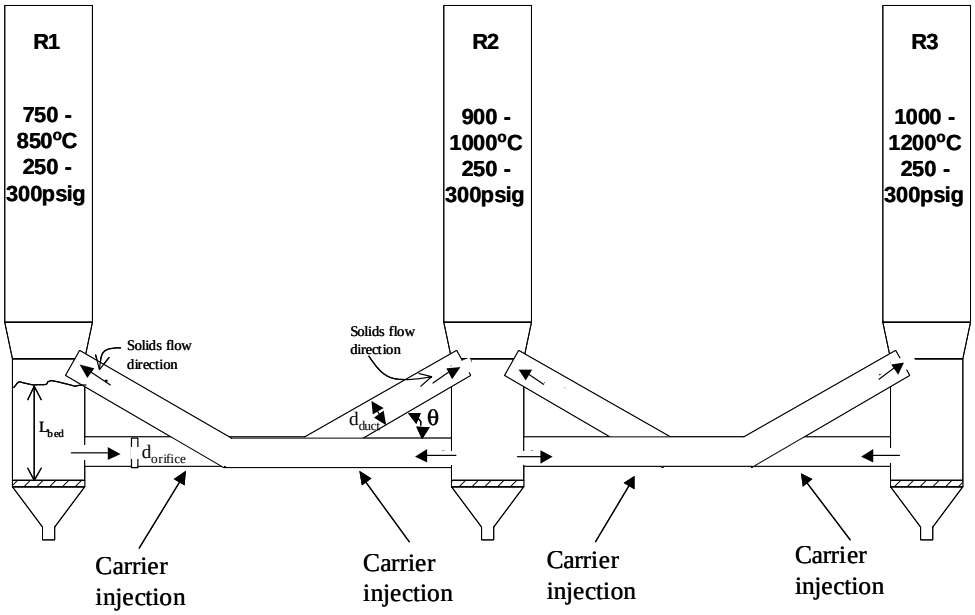

Figure 6-3. General schematic of the three-reactor system with solids transfer mechanism.

solids transfer in the ducts is provided in Figure 6-3.

The diameter of the intake duct is the main parameter that determines the mass flow rate of solids drawn from a reactor. This diameter must be designed to ensure that the flow of solids matches the design requirements. Equilibrium calculations were used to estimate the mass flow rate of solids required for continuous AGC operation.

Based on experimental observations, it is advisable to deliver the solids close to the top of the fluidized bed to avoid return flow of solids from the fluidized bed into the duct. Return flow of solids increases the amount of solids carrier gas required. The optimum location for delivery of solids is still being investigated and the results will be reported in the next Quarterly Technical Progress Report.

Based on these preliminary observations, a test matrix was developed using the following variables: fluidized bed height, intake orifice diameter, transport duct internal diameter, duct angle, and solids carrier gas flow rate. The mass flow rate of solids was measured as an indication of performance. The criteria for good solids transport include:

- Measured mass flow rate of solids approximates (less than 25% difference) the mass flow rate of solids obtained by gravity (open hole on the side of the fluidized bed).
- Carrier fluid flow rate is less than 50% of the fluidization flow rate.
- No solids accumulation is visible in the transport duct.
- The solid-fluid mixture is very dilute (more than 99% porosity) in the transfer duct.

During testing, the first two criteria were quantified and measured, while the 3rd and 4th were visually monitored via the transparent PVC ducts. A scale-up methodology has been developed to allow extrapolation of cold flow model results to actual pilot-scale conditions. This is especially important in scaling flow rates (both fluidization and solids transport).

6.4 Specification of Other Key Subsystems

The specifications for key subsystems have been developed and appropriate vendors have been located. Key subsystems include the boiler, superheaters, coal-feeding system, afterburner, scrubber and high-pressure air compressor. The majority of the equipment for the key subsystems has been ordered and will be delivered soon.

The boiler is a custom-built unit that will provide a maximum of 900 lb/hr of steam at 677ºC (1250ºF) and 350 psi. It is a stand-alone unit fully instrumented for safety and control. The superheaters are three 30 kW electric furnaces, one for each reactor. A coil will be located inside each furnace for superheating of process gas (steam or air) fed to each reactor. Several vendors have been identified, and the units will be ordered shortly.

The coal feeding system will consist of a Seepex progressive cavity pump that will be used to pump a mixture of coal and water from a 50-gallon reservoir. The pump can feed 12 gal/hr at 180 rpm.

The afterburner includes an Eclipse low-NO_x burner with a maximum firing rate of 1MMBtu/hr. It will fire natural gas along with AGC product gas and has been designed to produce less than 100-ppm of CO in the exhaust.

A spray tower scrubber has been designed to provide 90% efficiency of SO_2 removal for a 300-scfm process stream. The scrubber will remove SO_2 from the afterburner exhaust gas.

An Ingersoll Rand air compressor capable of delivering 22acfm of air at 500psig has been ordered to provide high-pressure air to the system. A 240-gallon high-pressure tank will also be used to provide storage and control of delivery pressure.

6.5 Preliminary P&ID

A process and instrumentation diagram has been developed, and is provided as Figure 6-4. The major equipment is shown, as well as all control and monitoring instrumentation. In addition to depicting the main reactors and the process streams, the location of instrumentation such as flow meters, control valves, thermocouples, pressure gauges and pressure regulators are shown. The P&ID will be used to guide pilot plant assembly efforts.

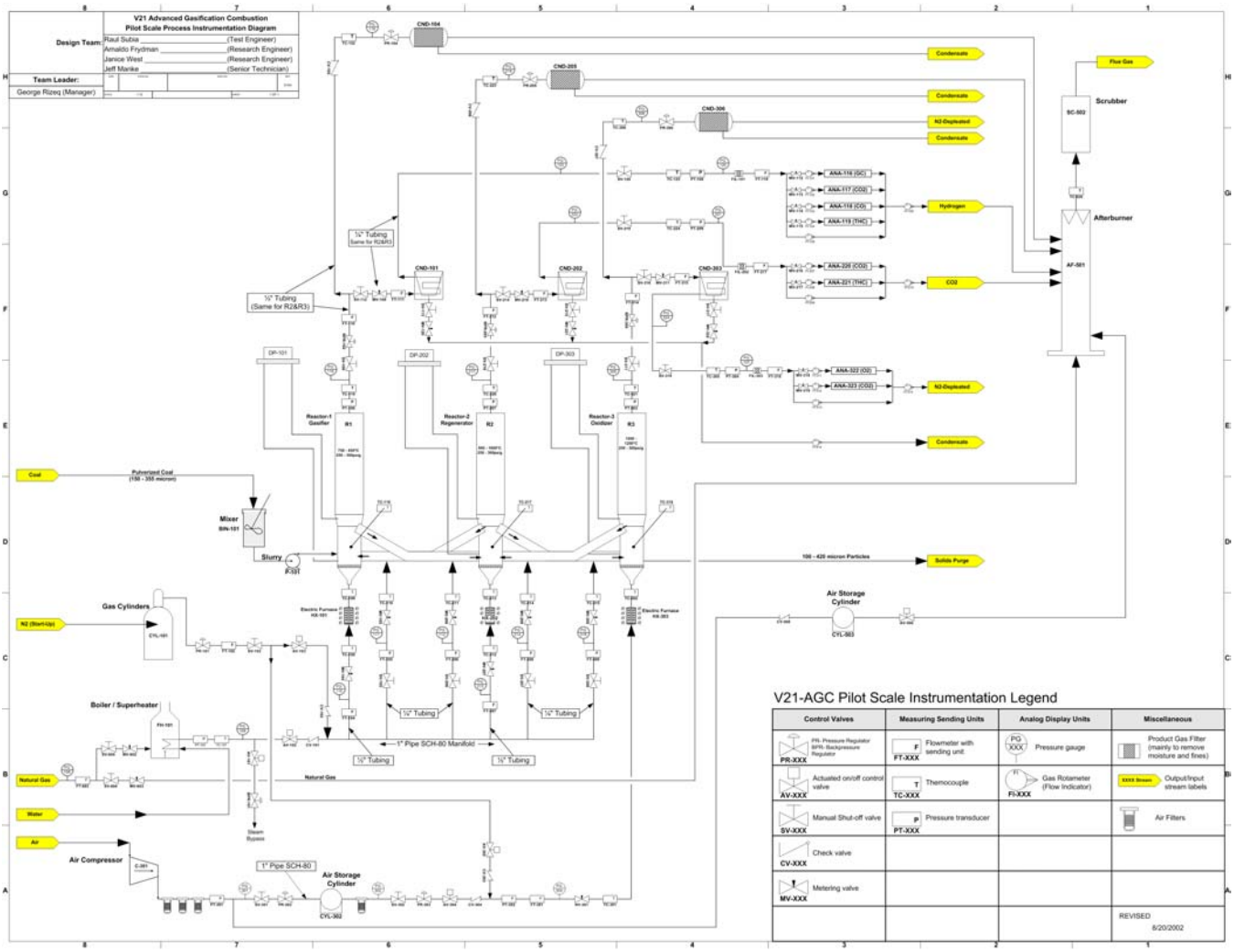

Figure 6-4. Process and Instrumentation Diagram (P&ID) for the pilot plant.

7.0 PILOT PLANT ASSEMBLY (Task 6)

The assembly of the pilot plant has been initiated in the last quarter. Reviews of key system and subsystem designs have been conducted. A system has been developed for tracking the status of ordered equipment, and plans have been put in place for the layout of the pilot plant to facilitate assembly by providing guidance on locating equipment as it arrives on site. Initial work has been conducted for the design of the data acquisition, control and safety system as well as the development of standard operating procedures.

7.1 Pilot-Scale System Equipment Floor Plan

The assembly of the pilot plant will be guided by the floor plan that was developed as part of Task 6. A preliminary scaled diagram of the proposed layout of the major equipment is shown in Figures 7-1 and 7-2. Figure 7-1 provides a top view of the floor plan, while figure 7-2 shows a side view with elevations of the major components and their support structures. The floor plan drawings will aid in system assembly and planning for piping and wiring needs.

8.0 SUMMARY AND CONCLUSIONS

Work conducted in this second program year has continued to develop the framework for demonstration of AGC process capabilities. Experimental data have been generated that validate the AGC concept and provide guidance for pilot-scale design and operation.

The lab-scale effort has included detailed kinetic investigations in a fixed bed reactor, and has recently been expanded to include high temperature and pressure fluidized bed experiments.

The bench-scale experimental efforts have focused on parametric testing to identify reasonable operating conditions for the pilot-scale system as well as provide information for validation of modeling efforts. The characterization of the three key AGC processes (coal gasification, CO_2 absorption/release, and OTM oxidation/reduction) has provided insight into the impact of operating conditions on H_2 yield and purity. Preferred operating conditions for Reactor 1 relative to CO_2 absorption and coal gasification have been identified. A detailed investigation into the behavior of OTM during reduction is currently near completion, and has involved a designed experiment that will identify the OTM reduction performance at a wide range of operating conditions and can be used in process modeling efforts.

The pilot-scale design effort has basically been completed, and major equipment and subsystems have been ordered. The reactor design has been finalized, based on heat transfer, fluidization, and process analyses. A preliminary P&ID has been developed, along with system layout drawings. Major subsystems have been specified and ordered, and a detailed safety analysis has been initiated.

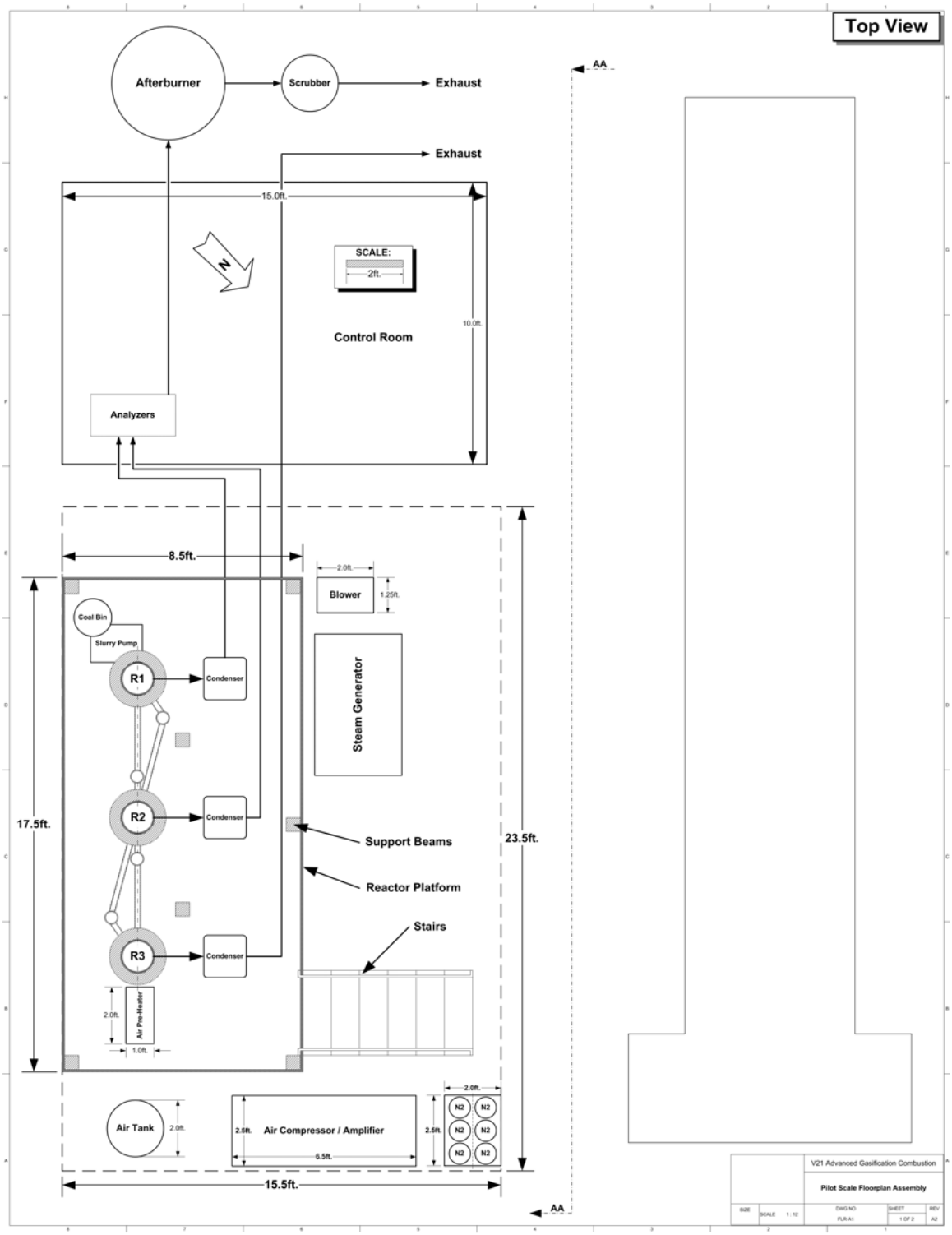

Figure 7-1. Pilot plant floor plan (top view).

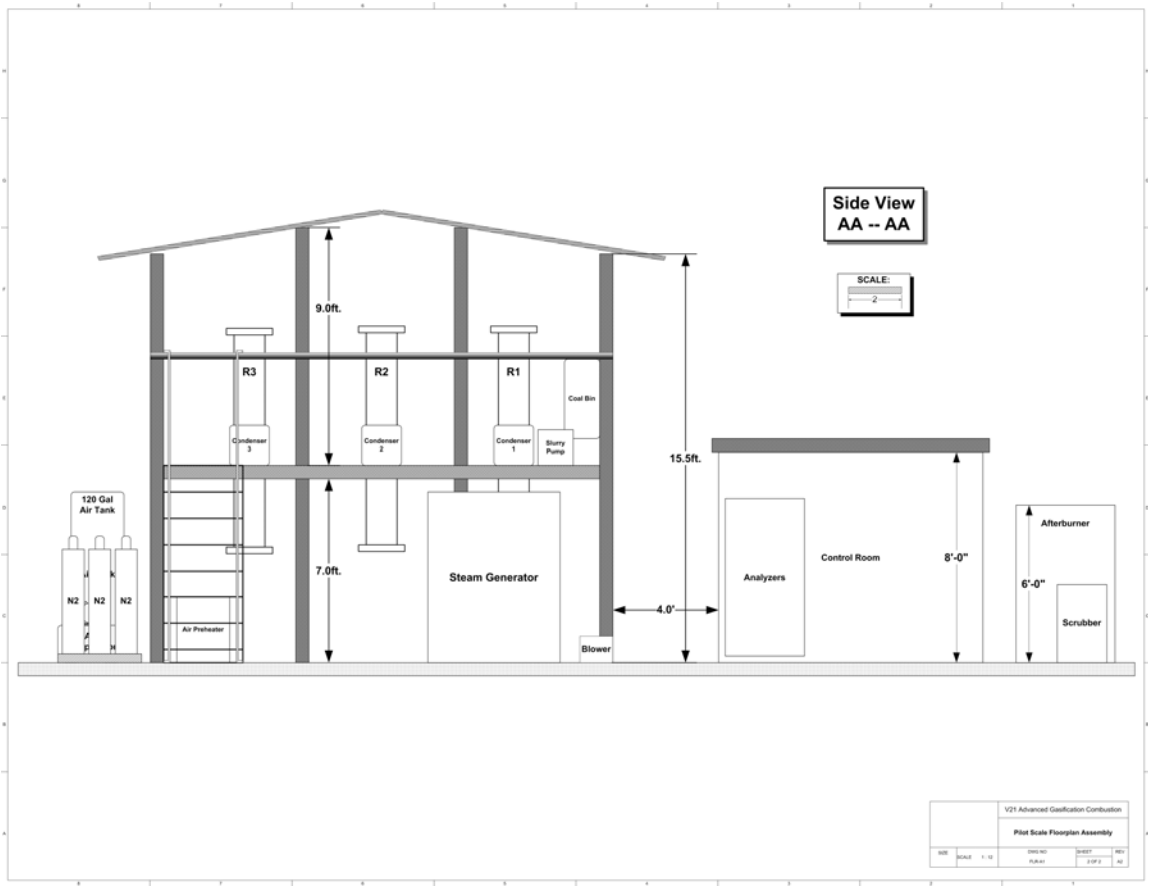

Figure 7-2. Pilot plant floor plan (side view).

9.0 FUTURE WORK

Additional bench-scale testing is planned to further investigate the performance issues related to the CAM and OTM bed materials, as well as possible interaction effects. In addition, the detailed testing of the Reactor 2 processes will be continued and expanded to provide further insight into the rates and mechanisms of char burnout, CO_2 release and OTM reduction processes.

Other continuing work on AGC technology development will include the assembly of the pilot-scale system, which will feature three fully-integrated circulating, fluidized bed reactors. In addition, progress will be made on modeling tasks in support of pilot-scale system operation. Integral to all these efforts is the continuing analysis of the economics and competitiveness of the AGC technology based on experimental and theoretical findings. These tasks will aid in ensuring that the technology is well established and that the AGC system will meet the needs of the power generation industry both efficiently and economically.

Task 1 Lab-Scale Experiments – Fundamentals
Task 1 activities will include experimental testing of the lab-scale high-temperature, high-pressure reactor and furnace. Kinetic tests involving coal, char, steam, air and combinations of oxygen-transfer material and CO_2 absorber material will be conducted. Cycling tests will also be

conducted. These experimental efforts will be closely coupled with the ongoing modeling efforts to ensure that the experiments will provide information useful in model validation.

Task 2 Bench-Scale System Design
This task has been completed.

Task 3 Bench-Scale Testing
Activities will focus on parametric testing to identify optimized operating conditions and specific tests to characterize material performance. Results of these tests will be used along with lab-scale results to modify and validate kinetic and process models, as well as provide inputs for economic evaluation efforts.

Task 4 Engineering and Modeling Studies
Kinetic and process models will be further developed and validated using results from testing activities. These models will also be used to provide information for pilot plant design efforts. Results obtained from the preliminary economic assessment will be used for identification of critical operating parameters that have significant impacts on the cost of electricity and hydrogen, and for recognition of limiting conditions from an economic standpoint.

Task 5 Pilot Plant Design and Engineering
This task has been completed.

Task 6 Pilot Plant Assembly
Future work on the pilot plant assembly will include a final design review. Other key subtasks include: finalizing the P&ID, tracking ordered items, inspecting manufactured parts, developing standard operating procedures, and designing the data acquisition interface. Finalizing the system layout is a key aspect of the assembly task. A plan will be developed for conducting shakedown testing of subsystems as they are installed, with special attention devoted to the safety and emergency shutdown systems and their integration with all equipment. The pilot plant will then be assembled and tested at EER's test site.

Task 7 Pilot Plant Demonstration
After the pilot plant is assembled, extensive shakedown testing will be conducted, with modifications made as needed. The operational evaluation of the AGC process with then proceed, followed by performance testing to identify the optimum H_2 yield that can be achieved with thorough analysis of the experimental data. A fuel flexibility study will be conducted to assess the impact of blending biomass fuels with coal.

Task 8 Vision 21 Plant Systems Analysis
The pilot plant performance will be used as the basis for the design of a preliminary full-scale Vision 21 module, along with consideration of plant integration issues. In addition, a more detailed economic and market assessment will be conducted, making use of the actual performance and design issues identified through the pilot plant demonstration.

Task 9 Project Management and Reporting
This is an ongoing task for the entire program.

10.0 PUBLICATIONS AND PRESENTATIONS

Team members have presented the AGC concept and progress at several conferences. These presentations and their subsequent publication in conference proceedings have generated interest in the AGC technology and helped in raising awareness of the DOE's Vision 21 program. Educating the technical sector and industry about this emerging technology will continue to be a priority as the program progresses. The presentations are listed below.

- George Rizeq, Raul Subia, Janice West, Arnaldo Frydman, Vladimir Zamansky, and Kamalendu Das, "Advanced Gasification-Combustion: Bench-Scale Parametric Study." *19th Annual International Pittsburgh Coal Conference*, Pittsburgh, PA, Sept 23-27, 2002

- George Rizeq, Janice West, Arnaldo Frydman, Raul Subia, and Vladimir Zamansky, Poster entitled: "Advanced Gasification-Combustion Technology for Utilization of Coal Energy with Zero Pollution." *29th International Symposium on Combustion*, Sapporo, Japan, July 22-26, 2002

- George Rizeq, Janice West, Raul Subia, Arnaldo Frydman, Vladimir Zamansky, and Kamalendu Das, "Advanced-Gasification Combustion: Bench-Scale System Design and Experimental Results," *27th International Technical Conference on Coal Utilization & Fuel Systems (Clearwater 2002)*, Clearwater, FL, March 4-7, 2002.

- R. George Rizeq, Ravi Kumar, Janice West, Vladimir Zamansky, and Kamalendu Das, "Advanced Gasification-Combustion Technology for Production of H_2, Power, and Sequestration," *18th Annual International Pittsburgh Coal Conference*, Newcastle, New South Wales, Australia, December 4-7, 2001.

- George Rizeq, Janice West, Arnaldo Frydman, Raul Subia, Ravi Kumar, Vladimir Zamansky and Kamalendu Das, "Fuel-Flexible Gasification-Combustion Technology for Production of Hydrogen and Sequestration-Ready Carbon Dioxide," *Vision 21 Program Review Meeting*, NETL, Morgantown, WV, November 6-7, 2001.

- R. George Rizeq, Richard K. Lyon, Janice West, Vladimir M. Zamansky and Kamalendu Das, "AGC Technology for Converting Coal to Pure H_2 and Sequestration-Ready CO_2," *11th International Conference on Coal Science* (ICCS), San Francisco, CA (Sept 30-Oct 5, 2001). NOTE: This conference was cancelled, but a proceedings volume was published.

- R. George Rizeq, Richard K. Lyon, Vladimir M. Zamansky, and Kamalendu Das, "Fuel-Flexible AGC Technology for Production of H_2, Power, and Sequestration-Ready CO_2," *26th International Technical Conference on Coal Utilization & Fuel Systems* (Clearwater Conference 2001), Clearwater, FL, March 5-8, 2001.